8-2005

Structure-Activity Relationship Studies on Thioxolone Compounds as Inhibitors of Human Carbonic Anhydrase II

Jared Nyabuto Orwenyo
Western Michigan University

STRUCTURE-ACTIVITY RELATIONSHIP STUDIES ON THIOXOLONE COMPOUNDS AS INHIBITORS OF HUMAN CARBONIC ANHYDRASE II

by

Jared Nyabuto Orwenyo

A Thesis
Submitted to the
Faculty of The Graduate College
in partial fulfillment of the
requirements for the
Degree of Master of Science
Department of Chemistry

Western Michigan University
Kalamazoo, Michigan
August 2005

ACKNOWLEDGMENTS

First of all I wish to express my sincere gratitude to my supervisor, Dr. Brian Tripp, for his guidance, patience and dedication throughout this entire research project. He allowed me to work under his tutelage and inspired me to explore science with energized vigor. I am also greatly indebted to my committee comprising Dr. David Reinhold, Dr.James Kiddle and Dr.Yirong Mo for their valued contributions and guidance. They brought me back in line when I seemed to stray away and ensured I stayed on course to achieve what I set off to do. I am also deeply grateful to Dr. Raymond Sung for his stimulating discussions and assistance with instrumentation.

I met and worked with many wonderful people along the way. Many thanks to the Tripp lab members who ensured there never was a dull day in the lab. Their moral support and suggestions are greatly appreciated. I also benefited from contributions from my fellow students from other labs and thank them for everything. Finally, I would like to thank my parents, David and Dorcas, for ensuring I had everything I ever wanted and supporting me in all my endeavors. I would also like to thank my brothers Kwame and Eddy, and sisters Caro and Eva, for being there for me at all times. Thank you for reminding me of the most important things in life. I could never have asked for more.

Jared Nyabuto Orwenyo

STRUCTURE-ACTIVITY RELATIONSHIP STUDIES ON THIOXOLONE COMPOUNDS AS INHIBITORS OF HUMAN CARBONIC ANHYDRASE II

Jared Nyabuto Orwenyo, M.S.

Western Michigan University, 2005

Carbonic anhydrase II (CA II) is a zinc metalloenzyme that catalyzes the reversible hydration of carbon dioxide. The role of this reaction in physiology has made it a target of many therapeutic approaches. Most CA II inhibitors currently known are sulfonamide-based and this is the only functional group incorporated into rationally designed CA II inhibitors. Thioxolone (6-hydroxy-1, 3-benzoxathiol-2-one), is a non-sulfonamide that has been found to have CA II inhibitory activity.

Thioxolone and its analogs were studied to evaluate the inhibition activity that can be achieved upon modification of the thioxolone molecule. IC_{50} values and dissociation constants were determined for thioxolone and its analogs and these were compared to those of potent sulfonamide drugs. Enzyme inhibition kinetics and other spectroscopic methods were used in an attempt to understand the mode of binding of thioxolone to CA II and the mechanism of inhibition. Results indicate a novel binding mode and enhancement of inhibition activity upon structural modification of thioxolone.

TABLE OF CONTENTS

Table of Contents-Continued

LIST OF TABLES

LIST OF FIGURES

CHAPTER I

INTRODUCTION

1.1 Background

Carbonic anhydrase was first reported by Meldrum and Roughton [1] who discovered the presence of an enzyme in erythrocytes that catalyzed the reaction:

$$CO_2 + H_2O \rightleftharpoons HCO_3^- + H^+ \quad (1)$$

The enzyme catalyzed the reaction in both directions and they named it carbonic anhydrase. The activity of this enzyme was found to be dependent on the metal zinc by Keilin and Mann.[2] Their work led to the conclusion that zinc was bound to the active site of carbonic anhydrase and was required for activity.

1.2 Human Carbonic Anhydrase II

This enzyme is one of the most efficient enzymes in nature. It is characterized by high activity with a turnover number for CO_2 hydration of 10^6 per second at 25 ° C and pH of 9.[3] It takes part in CO_2 transportation, acid-base regulation and bicarbonate secretion.[4] X-ray crystallography studies on CA II structure have revealed a deep active site cavity with a zinc ion bound at the bottom. The zinc-binding region is surrounded by a network of beta-sheet scaffolding and the zinc ion is bound to three histidine residues (His-94, His-96 and His-119) (Figure 1).

CA II Structure

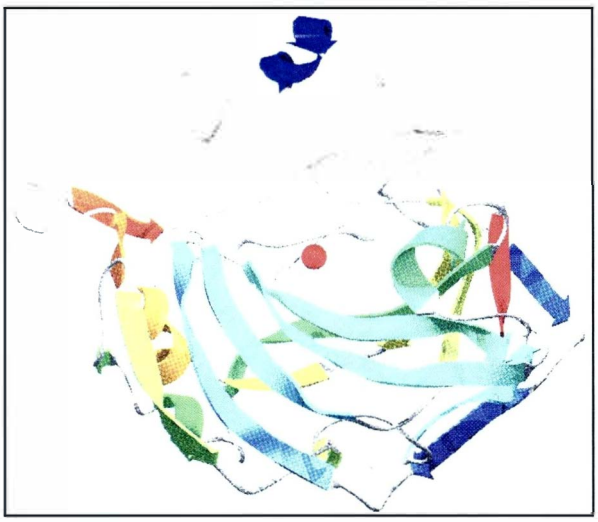

Figure 1. Ribbon diagram of human alpha-class carbonic anhydrase II enzyme structure. The red sphere shows the active site zinc ion. Image generated using PDB file 1A42.

Other residues that contribute to the structural integrity of the active site include Thr-199 and Glu-106.These form part of an extensive hydrogen-bonding network that aids in the mechanism of CO_2 hydration by optimizing the orientation needed for nucleophilic attack of CO_2 by the hydroxide. The hydroxyl group of Thr-199 also aids in product release by destabilizing its binding and is termed the door-keeper of the active site.[5]

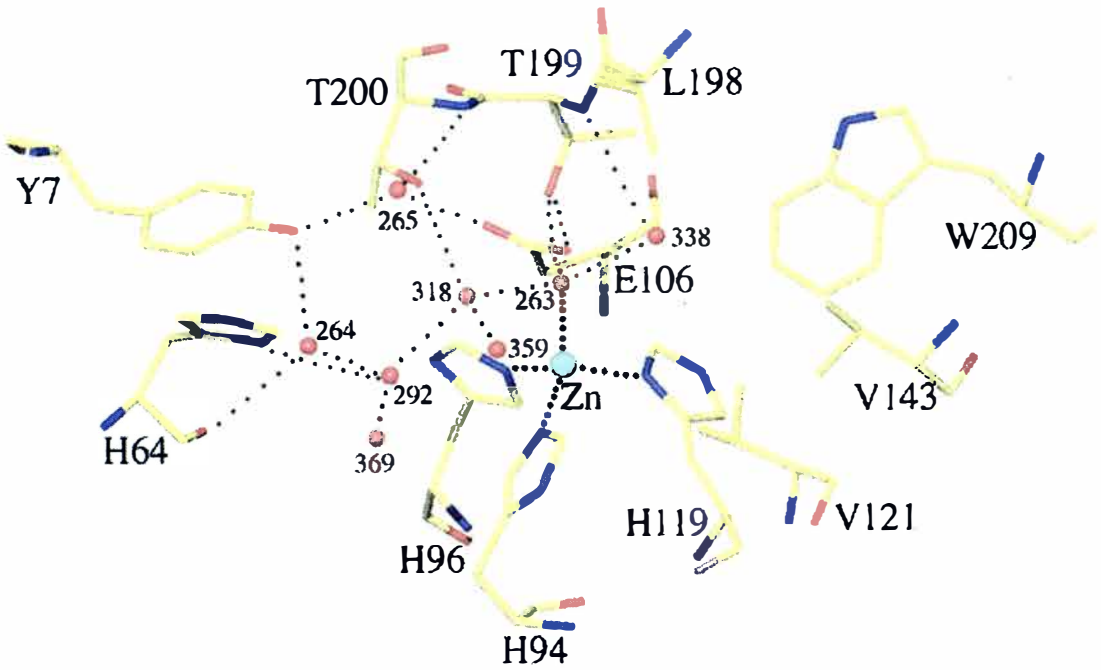

Figure 2. Human CA II active site. Red spheres represent water molecules and the large sphere represents the zinc ion. Ligand binding to zinc is represented by thick, dotted lines. Adapted from Huang et al, 2002 [6].

The mechanism of CA II hydration follows a consensus repertoire. A zinc-bound hydroxide ion acts as a catalyst in the interconversion of CO_2 to HCO_3^- and a water molecule is the resultant zinc ligand (Figure 3). A proton is then transferred from the water ligand to the imidazole ring of His-64 and is ultimately accepted by the solvent. The zinc-bound hydroxide that functions as the key active site species at the beginning of the catalytic cycle is thus regenerated.

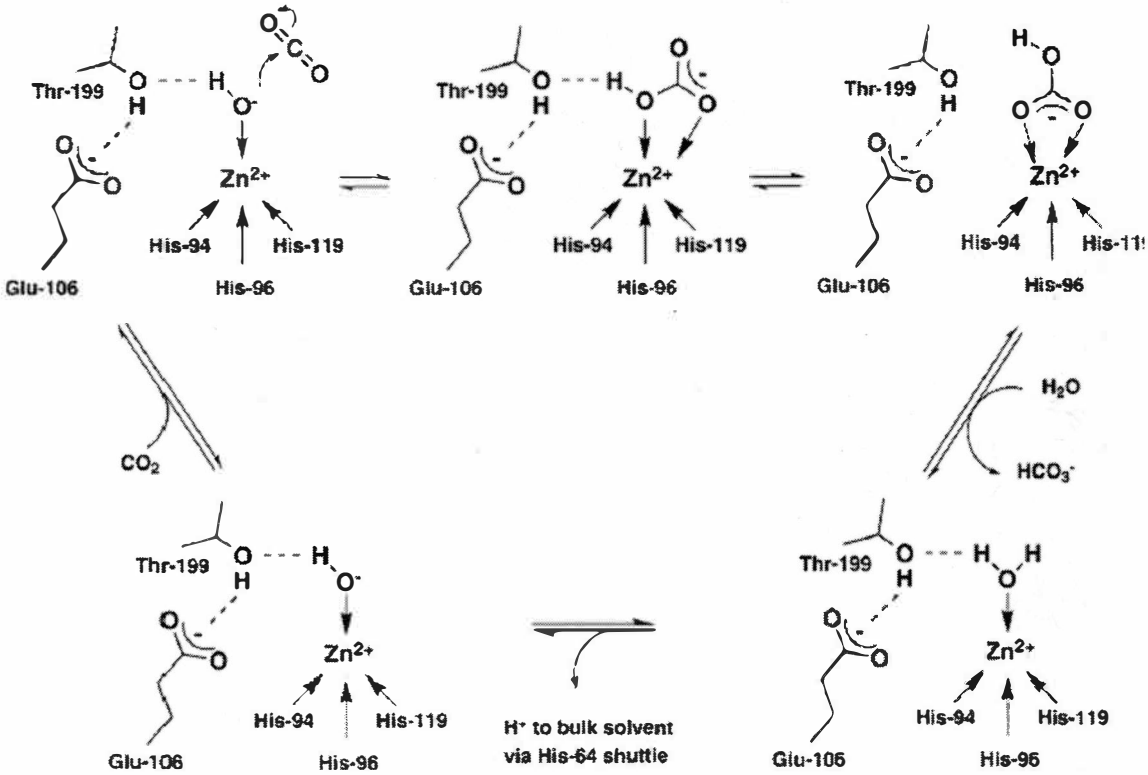

Figure 3. CO_2 hydration catalyzed by CA II. Adapted from Christianson and Cox, 1999 [7].

1.3 Carbonic Anhydrase

CA is prevalent in nature and this is evident in the many biological systems that exhibit its activity. CA has been shown to exist in all animals, plants and photosynthesizing organisms. Some non-photosynthesizing bacteria have also been exhibited CA activity. The universal occurrence of CA can be attributed to the basic but very important physiologic reaction it catalyzes:

$$Zn\text{-}H_2O \rightleftharpoons Zn\text{-}OH^- + H^+ \qquad (2)$$

$$Zn\text{-}OH^- + CO_2 \rightleftharpoons Zn\text{-}HCO_3^- + H_2O \rightleftharpoons Zn\text{-}H_2O + HCO_3^- \qquad (3)$$

The entire collection of CAs can be classified into 4 families with the common ones being α-, β- and γ- carbonic anhydrases. Evidence of the existence of a fourth family, the δ-CA, has been proposed but is not yet conclusive.[8] Lack of a primary sequence homology has precluded the possibility of a common ancestry therefore they are not evolutionarily related. However, all active sites have a zinc atom bound and some important sequences around the active site are conserved. Iron may be bound at some CA active sites, as shown in recent investigation involving γ-CA.[9] α-CAs are structurally monomers while the β- and γ-CAs are multimers.

Studies on the distribution of CAs in nature have shown that all CA in the animal kingdom belong to the α-family. α-CA activity has been shown to occur in the *Neisseria gonorrheae* species of bacteria.[10] β- CAs occur mainly in plants though some members have been identified in bacteria. The archaebacterium *Methanosarcina thermophila* accounts for the only γ-CA so far identified and characterized. [11] In addition to the reversible hydration of CO_2, CA has been shown to exhibit esterase [12] and oxonase [13] activities. Eleven active human α-CA isozymes designated I, II, III, IV, VA, VB, VI, VII, IX, XII and XV have been identified and characterized. [14]

Additionally, an acatalytic class of proteins similar to CA has been identified and its members are referred to as Carbonic Anhydrase Related Proteins (CARPs).This includes CAs VIII, X, XI and XIII. [14] The isozymes differ in tissue distribution and localization. More inherent differences are manifested in their catalytic properties and interactions with inhibitor molecules. CA I is mainly found in erythrocytes and the colon. CA II is found in many tissues such as erythrocytes,

kidneys and lungs. It is the most widely distributed isozyme in the human body. CA III occurs mainly in muscle and adipose tissues while the membrane-bound CA IV is found lungs and kidneys among other organs. CA IV is a mitochondrial enzyme while CA VI occurs in human saliva where it is thought to play a role in salivary pH regulation. CA II has been found to have the highest specific activity towards the reversible hydration of CO_2.[15] It is also the most studied and understood isozyme and much of what is known about CAs stems from studies carried out on CA II.

1.4 Carbonic Anhydrase Inhibition

The reaction catalyzed by carbonic anhydrase, though simple, plays a very important role in physiology making it an important target for pharmaceutical drugs. This is evident from the many therapeutic fields where CA inhibitors have already found use and in others where the potential is still being pursued. CA inhibitors have been used as diuretics [16; 17], antiglaucoma drugs [16; 18] and in the management of neurological disorders.[16] Their perceived role in tumor suppression is being investigated as a potential anticancer therapy.[16; 19] The CA isozyme expression profile has been suggested as a potential biomarker for gastrointestinal tumors.[14] Other uses being explored include treatment of osteoporosis and as a diagnostic tool in Magnetic Resonance Imaging (MRI) and Photon Emission Tomography (PET).[20]

The inhibition pattern of early CA inhibitors was found to follow that of other known metalloenzymes supporting the view that it indeed was a zinc

metalloenzyme.[21] Earlier uses of CA inhibitors were diuretics and most of the early inhibitors were sulfonamide-based drugs that had no specificity.

Other functional groups that have been proven to posses CA inhibitory activity include the sulfamate and hydroxamate groups. Sulfonamide-based drugs that are CA inhibitors include acetazolamide, methazolamide, ethoxzolamide, brinzolamide and dorzolamide used in the treatment of glaucoma. CA inhibitors used in treatment of glaucoma function by reducing intraocular pressure. This is accomplished by inhibition of CA in nonpigmented epithelial cells of the ciliary process thereby reducing aqueous humor formation and resulting in intraocular pressure reduction. Effective intraocular pressure reduction requires large doses of these sulfonamide drugs and this also results in a wide array of undesirable side effects including altered taste, malaise, fatigue, depression, anorexia, weight loss among a host of other side effects.[22; 23; 24; 25] This is a consequence of CA isozyme specificity by these drugs as they also inhibit CA in extraocular tissues. A significant fraction of the human population has shown an allergic reaction towards some sulfonamide-based drugs.[26; 27; 28]

To this end, attempts are being made to develop non-sulfonamide drugs for the many therapeutic areas in which sulfonamide are currently in use. The sulfonamide functional group, SO_2NH_2, has been recognized as essential in the aryl and heteroaryl sulfonamide classes of CA inhibitors due to the role it plays in coordination to the zinc atom in the enzyme's active site. Sulfonamides are known to bind to the zinc atom in CA as the anion, RSO_2NH^-. A departure from sulfonamide-

based drugs would entail the discovery of structural moieties with new modes of interaction with CA II.

Carbonic anhydrase inhibition has been studied for over six decades since 1940 when sulfanilamide (Figure 4), the first sulfonamide CA inhibitor, was discovered by Keilin and Mann. [21]

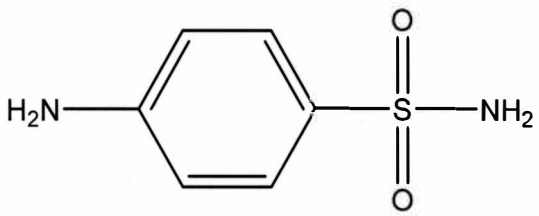

Figure 4. Sulfanilamide, the first sulfonamide CA inhibitor.

Further studies carried out on CA inhibition by sulfonamides revealed a decrease in CA carbon dioxide hydrase activity upon exposure to sulfonamides especially sulfanilamide which had been proven to be a potent inhibitor of CA.[21] These early studies on sulfonamide-CA complexes led to a conclusion that the sulfonamide group played a major role in the inhibition process while the amino group was important for therapeutic value but not inhibition. Additionally, the inhibitors were reported to be bound to the metal prosthetic group of the enzyme and the process was highly specific.[21]

A study comparing sulfanilamide and thiophene-2-sulfonamide concluded that the latter was more potent in its inhibition of carbonic anhydrase.[29] This was followed

by an extensive comparative study involving a series of o-, *p*-, N-substituted, aromatic, aliphatic and substituted sulfonamides and their IC_{50} values determined under varying conditions.[30] It had been suggested that heterocyclic compounds in which the sulfur atom of the unsubstituted sulfonamide group is attached to a carbon atom of the heterocyclic ring might possess inhibitory activity.

Since not many such molecules had been investigated, a series of heterocyclic compounds that were unsubstituted at the sulfonamide group were synthesized and tested for potency against carbonic anhydrase.[31; 32] Some of these compounds were found to be several hundred-fold times more active than sulfanilamide.[31]

Aliphatic sulfonamides are known to be weak CA inhibitors and by design, potent CA II inhibitors were expected to possess an aromatic or heteroaromatic ring. However, in a study involving the fluorinated derivative, $CF_3SO_2NH_2$, increased enhancement of potency on CA II inhibition was reported. [33] The search for newer CA inhibitors has mainly been confined to molecules that possess the sulfonamide moiety RSO_2NH_2 with numerous molecules being reported. [20; 34; 35; 36; 37; 38; 39; 40; 41; 42; 43; 44-45]

Carbonic anhydrase inhibition has been shown to involve simple anions [17; 45], dianions [46] and even larger molecules.[17; 18] Among the first known inhibitors of CA were potassium cyanate (KCN), hydrogen sulfide (H_2S) and sodium azide (NaN_3).[2] Anions have been found to be inhibitory and anionic inhibition of CA was shown to be non-competitive [47]. Those studied included fluoride (F^-), chloride (Cl^-), acetate (AcO^-), bromide (Br^-),nitrate(NO_3^-), iodide (I^-), and thiocyanate (CNS^-).[12] Cyanate

(NCO^-) was also shown to inhibit CA, albeit weakly.[48] The sulfate (SO_4^{2-}) dianion exhibited CA III inhibition activity in an uncompetitive manner as other dianions such as phosphate (HPO_4^{2-}) were shown to be activators.[49]

In a study on the effect of buffers on enzyme activity, imidazole was reported to inhibit CA I in a competitive manner in respect to its CO_2 hydrase activity.[3] Phenol was reported to be competitive inhibitor of CA II CO_2 hydrase activity. [50] Carbamoyl phosphate, a naturally occurring physiologically relevant molecule has also been found to inhibit the CA isozymes I, II and III.[51] A study involving N-unsubstituted carbamate esters with the structure $ROOCNH_2$ reported CA II inhibition.[52] These carbamate esters are commonly used as sedatives, anxiolytics and skeletal muscle relaxants.

Newer functional groups include molecules that possess the hydroxamate and sulfamate moieties.[53; 54] Sulfonylated amino acid hydroxamates with matrix metalloproteinase inhibitory activity have been shown to be potent CA inhibitors.[44] The results of this work on hydroxamates revealed a novel zinc-binding functionality, the SO_2NHOH group. CA II inhibitory studies on topiramate, a novel sugar sulfamate used for treatment of epilepsy and migraine, showed that it was a moderate CA II inhibitor.[55; 56] This activity was attributed to its sulfamate group, $ROSO_2NH_2$. In this same study, a sulfamide analogue of topiramate possessing the $RNHSO_2NH_2$ sulfamide moiety was also investigated and was found to be a much weaker inhibitor of CA II compared to topiramate.

1.5 Model Compound: Thioxolone

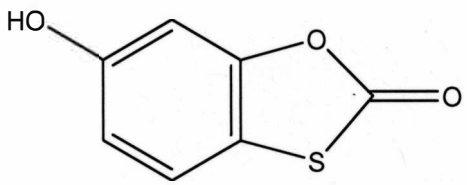

Figure 5. 6-hydroxy-1, 3-benzoxanthiol-2-one (thioxolone).

Thioxolone, 6-hydroxy-1, 3-benzoxanthiol-2-one, has a molecular mass of 168.16 Da (Figure 5). Its structure, with a hydrogen-bond donor group (hydroxyl) on one end and an acceptor group (carbonyl) on the other end, allows for the formation of extensive hydrogen bonds.[57] Thioxolone has not been described as a carbonic anhydrase inhibitor, and this work aims to be the first attempt to characterize thioxolone as a CA II inhibitor.

It lacks the sulfonamide, sulfamate or related functional groups, moieties that have been found to occur in CA inhibitors.Thioxolone has found wide use in medically related applications. It has been found to possess medicinal properties making it useful for skin conditions such as acne. [58] Other reported medically-useful properties include cytostatic [59] , antipsoriatic, antibacterial and antimycotic activity.[60]Some hair-care products such as shampoos have been able to incorporate thioxolone into their formulation as an anti-seborrheic agent. This has been attributed

to its oil-regulatory and antibacterial activity. Thioxolone toxicity has been connected to cases of contract dermatitis [61].

1.6 Preliminary Studies: X-ray Crystallography

A research collaborator, Dr. Robert McKenna at the University of Florida, carried out a preliminary study entailing X-ray crystallography of CA II and thioxolone. Analysis of the preliminary X-ray diffraction data showed four thioxolone hydrolysis products bound at or near the CA II active site. These included three 4-mercaptobenzene-1, 3-diols and one dihydroxyacetone molecule (Figure 6).

Protein crystals have a high solvent content and in this structure 211 solvent molecules were observed. Inferences that can be made from these results suggested that thioxolone undergoes hydrolysis into ester products mainly identified as 4-mercaptobenzene-1, 3-diol. However, this hydrolysis could also be an artifact from the high intensity x-ray radiation source at Cornell University used for the diffraction studies.

These results also revealed the potential existence of 2-3 unique binding sites within the CA II active site where the thioxolone hydrolysis products could bind. An additional molecule resembling dihydroxyacetone was evidently bound to the CA active site adjacent to the bound 4-mercaptobenzene-1, 3-diol. CA II inhibitors have been known to bind to the zinc atom at the active site via nitrogen atoms as negatively charged groups. In this preliminary study, one of the thioxolone hydrolysis products appeared to be bound to the active site zinc atom via a thiol group, while two other

product molecules were bound near the entrance to the active site region, in an oxidized disulfide-linked form.

The first molecule bound to the zinc ion may represent a novel mode of binding by CA inhibitors, although thiols are well known as zinc ligands in other metalloproteins, such as zinc finger DNA-binding domains in transcription factors and the beta-class carbonic anhydrases. This possible novel binding mode guided the pursuit of thiol group-containing aromatic compounds in this study and their comparison to known sulfonamide CA II inhibitors.

Figure 6. Preliminary X-ray crystal structure of thioxolone hydrolysis products bound to CA *II* active site. A molecule of 4-mercapto-benzene-1, 3-diol appears to be bound via a *thiol* bond to the zinc ion. A *molecule* of dihydroxyacetone appears to be bound nearby in the active site region. The central orange sphere is the active site zinc ion. Figure prepared using unpublished coordinates determined by Dr. McKenna, University of Florida. Coordinates were provided, courtesy of Dr. Robert McKenna, University of Florida.

Hydroxamate inhibitors of CA have been reported to bind CA II in a novel manner involving the direct coordination of the ionized nitrogen atom to zinc.[53] Rema Iyer, a previous WMU Biological Sciences M.Sc. student, performed a screen of 960 compounds in the Genesis Plus library (Microsource Discovery Systems, Inc., Gaylordsville, CT) for inhibitors of human CA II. Along with various sulfonamide compounds, several novel inhibitors were identified, including thioxolone (Fig. 5).

This, being a non-sulfonamide, thioxolone and its analogs may offer an insight into the design of better CA II inhibitors, devoid of the sulfonamide moiety. This research is an attempt to investigate and define the mechanism of action and Structure-Activity Relationships (SARs) of thioxolone and related compounds with a view it may lead to useful relationships between structure and activity of these compounds.

CHAPTER II

MATERIALS AND METHODS

2.1 Enzyme Expression and Purification

The CA II enzyme was a gift from Dr. Carol Fierke of the University of Michigan. Encoded in the T7 promoter plasmid pACA, the enzyme was expressed in the BL21 (DE3) strain of *E. coli* and these bacterial cells were grown in a culture containing Luria-Bertani medium at 37° C with shaking at 225 rpm. Upon attaining an optical density at 600 nm of 0.5-0.8, induction was performed by addition of isopropy-beta-D-thiogalactopyranoside (IPTG) (1μl/ml) for three hours. The cells were then resuspended in 20 mM Tris buffer, pH 7.5 and lysed by addition of 1.0 mg/ml lysozyme, 5 μg/ml DNase I and 5 mM $MgSO_4$, while stirring on ice for 30 minutes.

Centrifugation at 8000 x g was performed to achieve clarification and then an SP Sepharose Fast Flow cation exchange column was used to separate the protein. A 0-1.0 M NaCl gradient was applied to elute the CA II from the column and upon collection, the protein was concentrated using Amicon/Millipore Centricon centrifugal concentrators with a YM-10 membrane. The pure CA II aliquots were frozen in glycerol and stored at -80° C. Upon SDS PAGE analysis, the CA II was found to have more than 95% purity. The enzyme concentration was determined using $5.4 \times 10^4\ M^{-1}cm^{-1}$ as the molar absorptivity constant.

2.2 Thioxolone, Analogs and Other Sulfonamides

Thioxolone is commercially available and pure analytical grade thioxolone was purchased from Sigma Aldrich. The thioxolone analogs (Figure 7) were sourced from Specs (Delft, Netherlands). The compound selection was tailored to heterocyclic compounds with a sulfur atom and lacking a sulfonamide group. The compounds had a structural similarity to thioxolone with different side chains. Another batch of three analogs (Figure 8) was synthesized by Dr. James Kiddle at Western Michigan University and these were also assayed for CA II inhibitory activity.

As part of a separate collaboration project with Dr. Daniel Ketcha of Wright State University in Dayton, Ohio, a series of 19 novel sulfonamide compounds (Figure 9) and precursors synthesized in his laboratory were analyzed in our laboratory for CA II inhibition activity. These compounds were screened for inhibition activity using the esterase assay and the results are also discussed in this research thesis.

2.3 Inhibition studies

Carbonic anhydrase has been found to possess esterase activity and this has provided a reliable assay for its activity.[12] The CA-catalyzed hydrolysis of *p*-nitrophenyl acetate results in the liberation of the *p*-nitrophenolate anion with an isosbestic point at 348 nm (Figure 10). The rate of production of the anion is directly related to the disappearance of the substrate. In this study, a series of inhibitor concentrations were tested for inhibitory potency and the IC_{50} were values computed

Specs Compounds

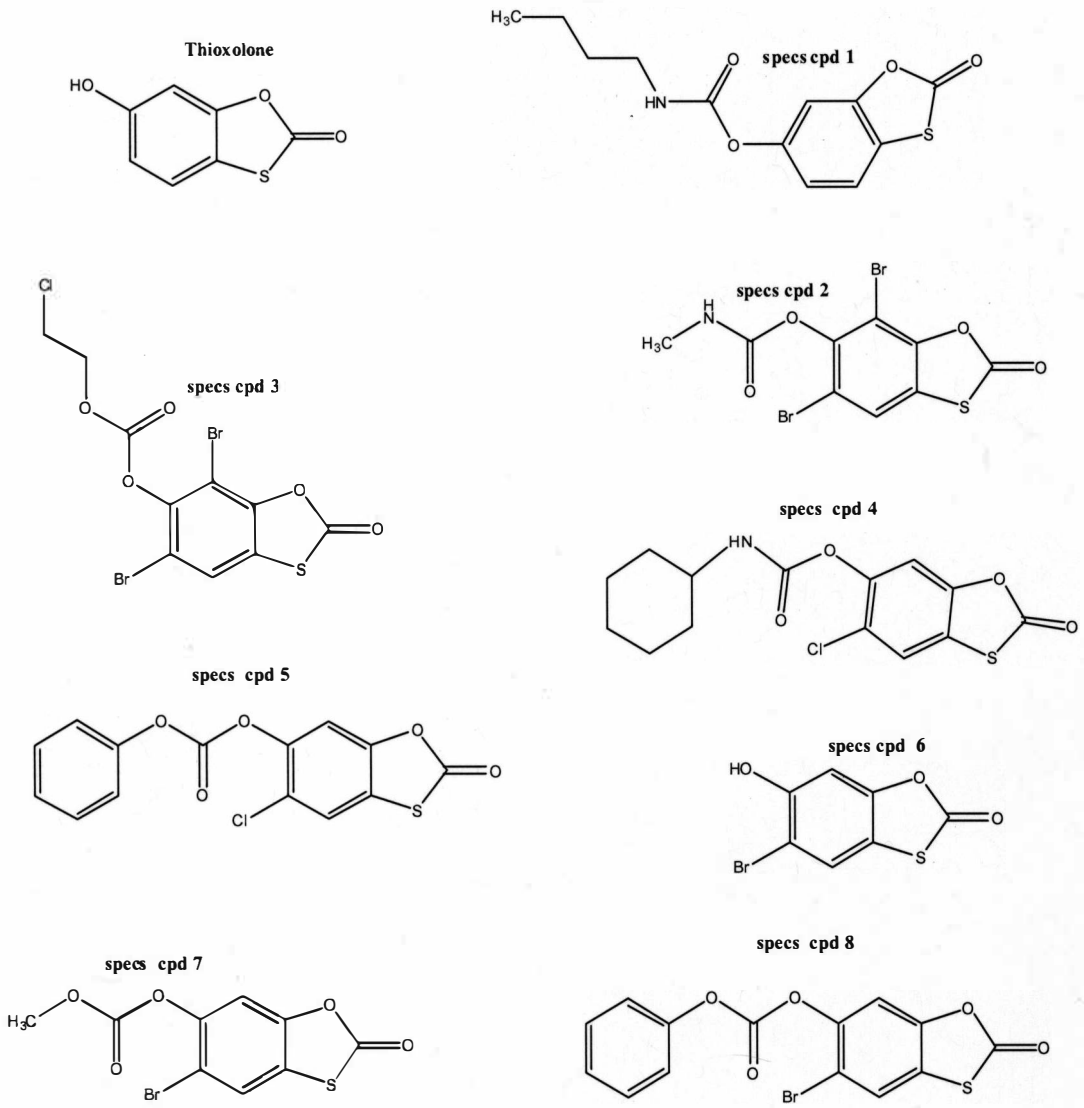

Figure 7. Thioxolone and analogs.

specs cpd 9

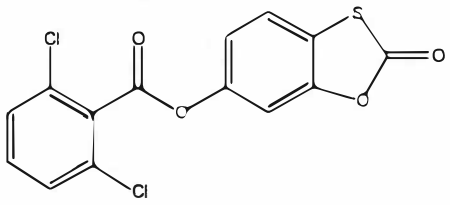

specs cpd 10

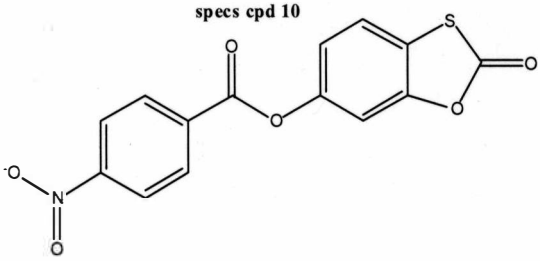

specs cpd 11

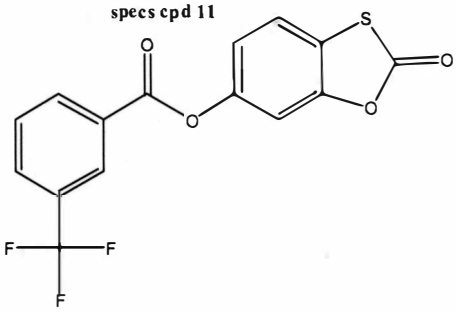

specs cpd 12

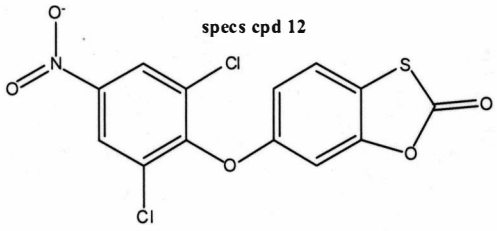

2-Mercaptophenol

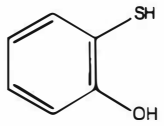

specs cpd 13

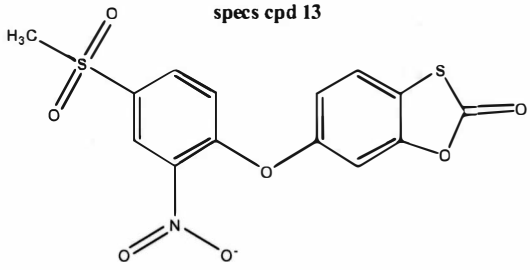

Benzenethiol

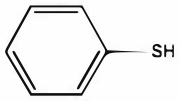

Methazolamide

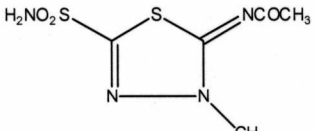

(Sulfonamide)

Acetazolamide

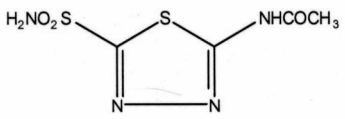

(Sulfonamide)

Figure 7 (cont.)

Analogs from Dr. James Kiddle

Compound 1

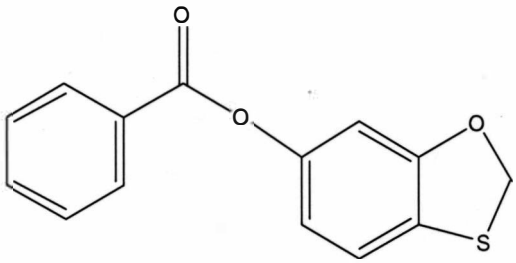

Compound 2

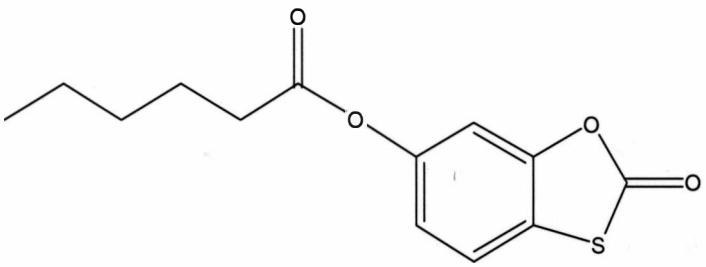

Compound 3

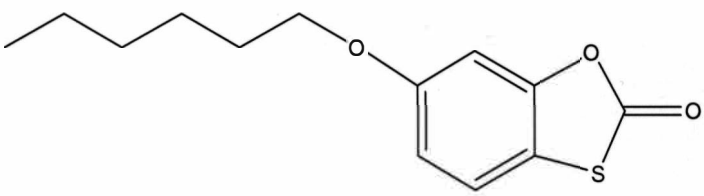

Figure 8. Thioxolone analogs acquired from Dr.James Kiddle's lab.

Wright State Compounds

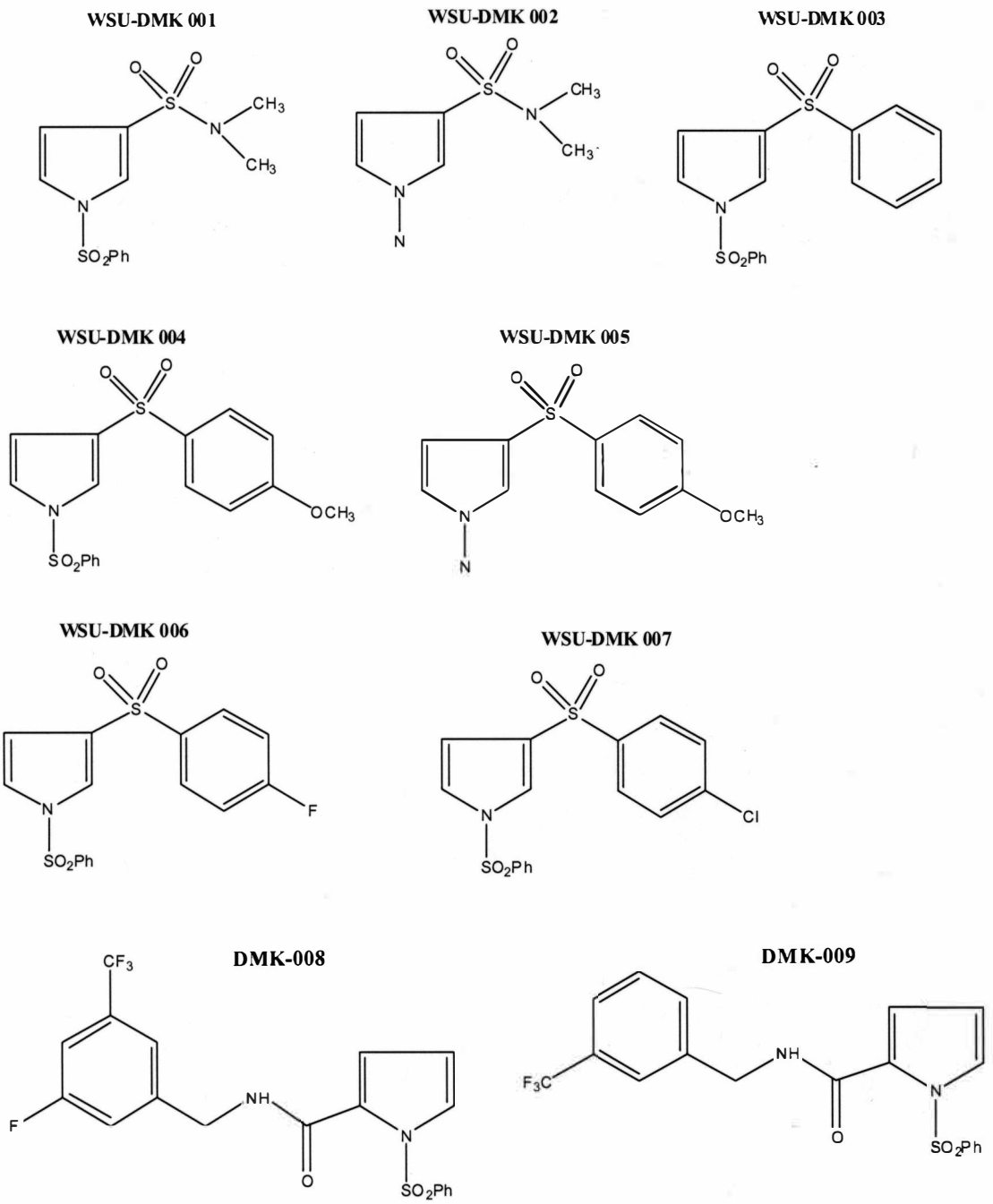

Figure 9. Compounds acquired from Wright State University.

DMK-010

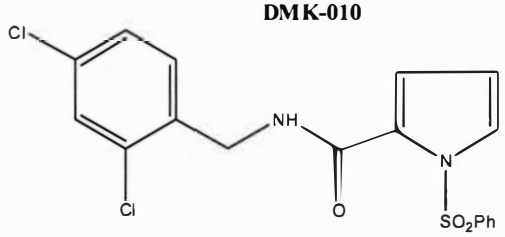

DMK-011

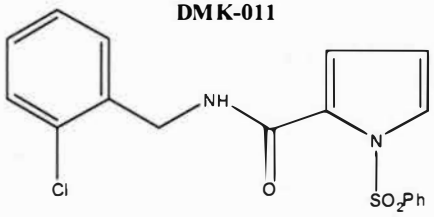

DMK-012

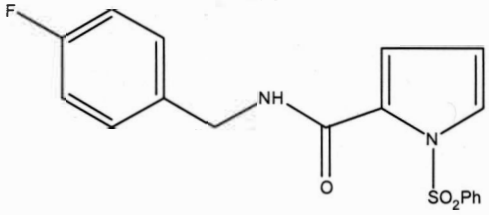

DMK-013

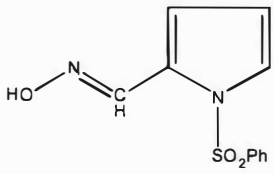

DMK-014

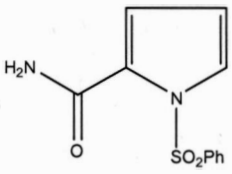

DMK-015

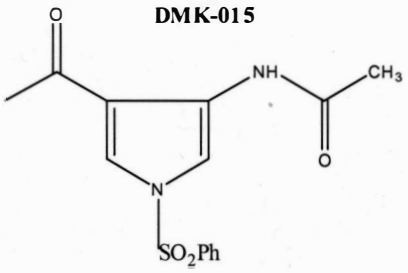

DMK-016

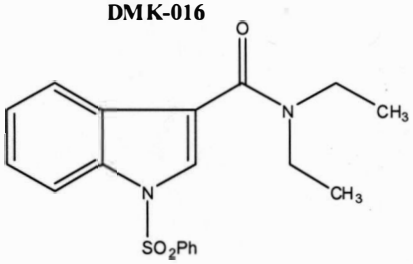

DMK-017

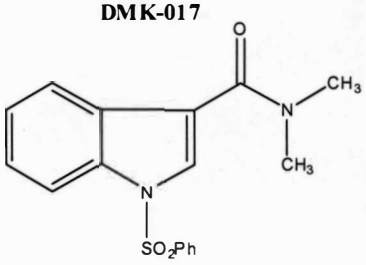

DMK-018

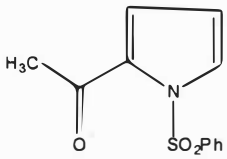

DMK-019

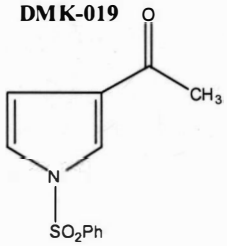

Figure 9 (cont.)

IC_{50} values are defined as the molar concentrations of inhibitor required to inhibit 50 percent of enzymatic activity. A limiting concentration of enzyme was titrated against increasing concentrations of inhibitors. The concentrations of inhibitors were achieved through a process of serial dilution in 96-well storage plates. Inhibitors were dissolved in DMSO to achieve a starting concentration of 10 mM and 100 µl aliquots were dispensed in duplicate into the first column wells. Aliquots of 50 µl of DMSO were dispensed into columns 2-11. A 1:2 dilution was carried out as follows: 50 µl aliquots were transferred from the first column containing the 10 mM inhibitor solution into the following column and upon mixing, another 50 µl aliquot was transferred to the next column and this was continued across a second plate that also had controls in column 12.

Column 12 was the control column and the first four rows contained 50 µl aliquots of 10 mM acetazolamide inhibitor (positive controls) and the last four rows contained 50 µl aliquots of DMSO (negative controls). These were the compound source plates. The dilutions were performed across columns 2-11, thus avoiding the controls in column 12. This resulted in a series of concentrations as shown in table 1.

CA II enzyme was diluted with 50 mM pH 7.5 MOPS buffer, 33 mM Na_2SO_4 and 33 mM EDTA. Aliquots of 100 µl each were then dispensed into 96 well optical plates using a programmable 8-channel pipette (Matrix P1250). This was calculated to give a final enzyme concentration of 1 mM per well upon addition of inhibitor and substrate.

Table 1

Inhibitor Concentrations in 96-Well Plate Format

Column Per well	Final Inhibitor Concentration (Molar)	Column	Final Inhibitor Concentration Per well (Molar)
1	9.00×10^{-5}	13	4.40×10^{-8}
2	4.50×10^{-5}	14	2.20×10^{-8}
3	2.25×10^{-5}	15	1.10×10^{-8}
4	1.13×10^{-5}	16	5.50×10^{-9}
5	5.63×10^{-6}	17	2.75×10^{-9}
6	2.82×10^{-6}	18	1.37×10^{-9}
7	1.41×10^{-6}	19	6.87×10^{-10}
8	7.04×10^{-7}	20	3.44×10^{-10}
9	3.52×10^{-7}	21	1.72×10^{-10}
10	1.76×10^{-7}	22	8.60×10^{-11}
11	8.80×10^{-8}	23	4.30×10^{-11}
12	Controls	24	Controls
Final assay volume = 111 µl			

Aliquots of 1 µl of inhibitor were dispensed using a 96-channel programmable liquid handling workstation (Plate Trak, CCS Packard, Torrence, CA) from the source plates into the 96-well polystyrene optical plates (Costar) containing CA II in buffer and the reaction mixture was allowed to equilibrate for 20 minutes at room temperature with gentle stirring.

The *p*-nitrophenyl acetate was added in 10 µl aliquots to each well using a multi-drop instrument (Labsystems, Finland) and this was calculated to give a final concentration of 500 µM per well. The hydrolysis of *p*-nitrophenyl was monitored by the appearance of the nitrophenolate anion at 348 nm using a Specramax (Molecular Devices, Sunnyvale, CA) spectrophotometer equipped with a 96-well plate reader set in the kinetic mode. Spectra were collected at 0.15 s intervals for 5 minutes.

The data collected was transferred from the spectrophotometer program into Microsoft Excel format and the percent inhibition was computed as a function of concentration. This data was fitted using the Graphpad Prism (Version 4.0) graphing software to yield the IC_{50} values for thioxolone and related compounds.

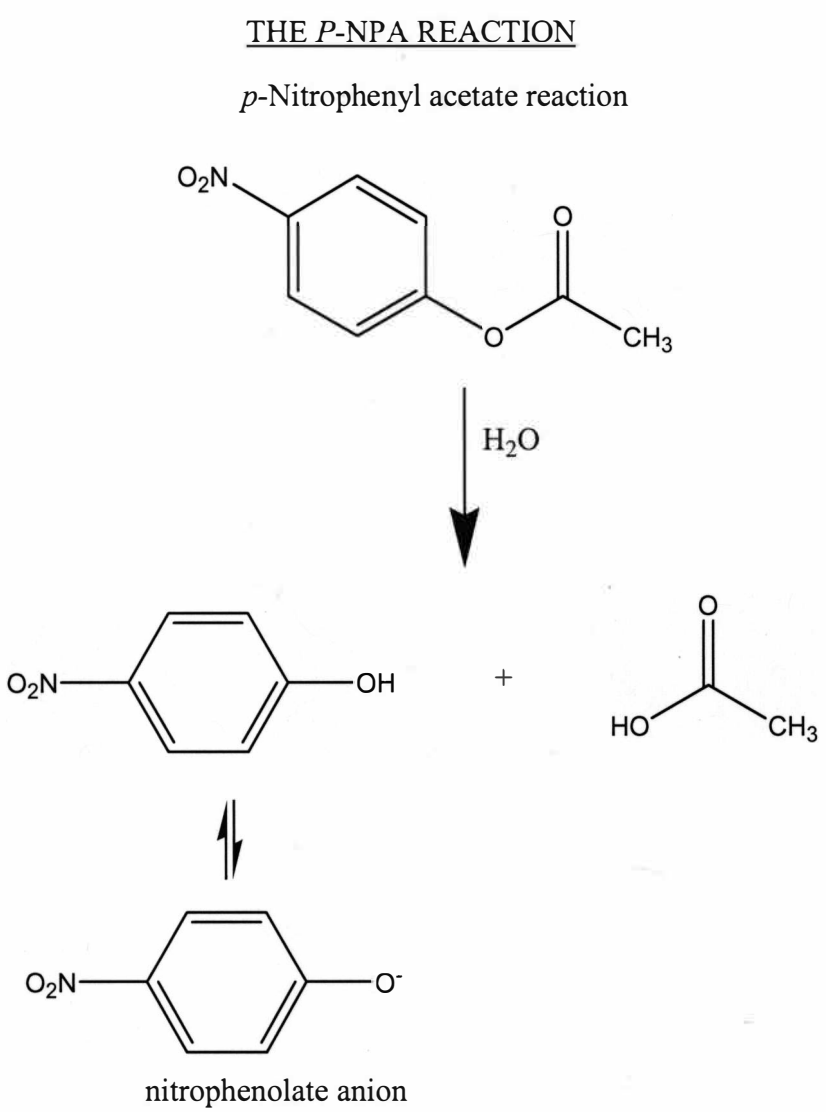

Figure 10. Hydrolysis of *p*-nitrophenyl acetate by CA II

2.4.1 Dissociation Constant Determination

Dansylamide is a fluorescent dye with an emission spectrum that is sensitive to the environment and exhibits weak fluorescence in aqueous solutions. A perturbation in the local environment leads to changes in its spectrum and this has been used extensively in protein structural studies. Ligand binding may lead to changes in solvation and this in effect may change the fluorescence properties of dansylamide.[62]

Dansylamide is relatively non-fluorescent until it binds to hydrophobic regions in proteins and this property has enabled it to be used as a probe for protein-ligand binding studies. When bound to protein, dansylamide exhibits environment sensitive fluorescence quantum yields and emission maxima accompanied by Stokes shifts. In one of the early studies with CA, dansylamide was used as a probe and its properties led to the proposition of a highly hydrophobic pocket at the CA active site.[63]

In this study, the dansylamide dissociation constant for CAII was determined and based on competition for the binding site with inhibitors, the inhibitor dissociation constants for CA II were also determined. This was based on the dansylamide displacement method used to study the CA II binding site.[63; 64] Because the spectral changes would be subject to the nature of the enzyme, buffer composition, buffer pH and stability of dansylamide in the reaction mixture, emission spectra were acquired both the presence and absence of CA II and in the presence of thioxolone, all in a standard buffer of pH 7.5 containing 50 mM MOPS, 33 mM Na_2SO_4 and 33 mM EDTA.

The dansylamide dissociation constant was determined by titrating increasing concentrations of dansylamide with a limiting CA II concentration in MOPS buffer. The different concentrations of dansylamide were achieved by serial dilutions in 96-well storage plates starting with a 10 mM stock solution of dansylamide in DMSO. Aliquots of 100 µl of the 10 mM stock solution were dispensed into the first column. Aliquots of 50 µl of DMSO were then dispensed into the remaining 11 columns and a 1:2 dilution carried out using a multi-channel pipette to ensure transfer of equal volumes.

Aliquots of 50 µl were transferred from the first column containing the 10 mM dansylamide solution into the following column and upon mixing, another 50 µl aliquot was transferred to the next column and this continued across a second plate. Thus, two plates which served as the source plates. This resulted in a wide range of dansylamide concentrations (Table 2).

CA II was added to MOPS buffer to attain a final enzyme concentration of 1 µm per well. Upon mixing and equilibration, 100 µl aliquots of the enzyme solution were dispensed into 96-well optical plates using a multi-channel pipette. Aliquots of 1 µl dansylamide solution were dispensed from the dilution source plate into the 96-well fluorescent plate (Costar) plate containing CA II using a 96-channel programmable liquid handling workstation (Plate Trak, CCS Packard, Torrence CA) and the reaction mixture allowed to equilibrate for twenty minutes at room temperature with gentle stirring.

The fluorescence spectra were then recorded using a Fluostar fluorimeter (BMG Labtechnologies, Germany), with excitation wavelength set at 280 nm and emission wavelength set at 470 nm.

Table 2

Dansylamide Concentrations in 96-Well Plate Format

Column	Final Concentration Per well (mM)	Column	Final Concentration Per well (mM)
1	9.901×10^{-2}	13	2.417×10^{-5}
2	4.990×10^{-2}	14	1.209×10^{-5}
3	2.475×10^{-2}	15	6.043×10^{-6}
4	1.238×10^{-2}	16	3.022×10^{-6}
5	6.188×10^{-3}	17	1.511×10^{-6}
6	3.094×10^{-3}	18	7.554×10^{-7}
7	1.547×10^{-3}	19	3.777×10^{-7}
8	7.735×10^{-4}	20	1.888×10^{-7}
9	3.868×10^{-4}	21	9.442×10^{-8}
10	1.934×10^{-4}	22	4.721×10^{-8}
11	9.669×10^{-5}	23	2.361×10^{-8}
12	4.834×10^{-5}	24	1.180×10^{-8}
Final assay volume = 101 μl			

A gain setting of 100 was applied. This was done to allow for optimal signal: noise ratio and was achieved by using the wells with expected maximum fluorescence (column 1) to calibrate the fluorimeter. The dansylamide binding constant and error estimates were determined using Graphpad Prism curve-fitting program using equation 3 below.[64]

$$\text{fraction } F_{total} = \frac{F_{obs} - F_{ini}}{F_{end} - F_{ini}} = \frac{1}{1 + K_{DNSA}/[DNSA]} \quad (3)$$

F_{total} represents the total fluorescence

F_{obs} represents the observed fluorescence (fluorescence observed in a well with a given dansylamide concentration)

F_{ini} represents the initial fluorescence of the protein devoid of dansylamide binding (minimum fluorescence)

F_{end} represents the fluorescence end point (maximum fluorescence)

K_{DNSA} represents the dansylamide dissociation constant

[DNSA] represents the dansylamide concentration in a plate well

2.4.2 Inhibitor Dissociation Constant Determination

Dansylamide has been found to bind CA at the same site as sulfonamide inhibitors and competition for binding to this site was evident by quenching of dansylamide-induced fluorescence when sulfonamide inhibitors bind to the same CA molecule.[63] This competition for CA II binding between dansylamide and inhibitor was the basis for the inhibitor dissociation constant determination.

A mixture containing a fixed concentration of dansylamide and CA II was titrated against increasing inhibitor concentrations. The concentrations of inhibitors were achieved through a process of serial dilution on 96-well plates (Costar). Inhibitors were dissolved in DMSO to achieve a starting concentration of 10 mM and 100 µl aliquots were dispensed in duplicate into the first column.

Aliquots of 50 µl of DMSO were dispensed into columns 2-11. A 1:2 dilution was carried out as follows: 50 µl aliquots were transferred from the first column containing the 10 mM inhibitor solution into the following column and upon mixing, another 50 µl aliquot was transferred to the next column and this continued across two plates. Column 12 was the control column and the first four rows contained 50 µl aliquots of 10 mM acetazolamide inhibitor (positive controls) and the last four rows contained 50 µl aliquots of DMSO (negative controls). The dilutions were carefully done so as to avoid the control columns. This resulted in a series of concentrations as follows:

Table 3

Inhibitor Concentrations in 96-Well Plate Format

Column	Final Inhibitor Concentration Per Well (millimolar)	Column	Final Inhibitor Concentration Per Well(millimolar)
1	9.901×10^{-2}	13	4.834×10^{-5}
2	4.990×10^{-2}	14	2.417×10^{-5}
3	2.475×10^{-2}	15	1.209×10^{-5}
4	1.238×10^{-2}	16	6.043×10^{-6}
5	6.188×10^{-3}	17	3.022×10^{-6}
6	3.094×10^{-3}	18	1.511×10^{-6}
7	1.547×10^{-3}	19	7.554×10^{-7}
8	7.735×10^{-4}	20	3.777×10^{-7}
9	3.868×10^{-4}	21	1.888×10^{-7}
10	1.934×10^{-4}	22	9.442×10^{-8}
11	9.669×10^{-5}	23	4.721×10^{-8}
12	Controls	24	Controls
Final assay volume = 101 µl			

A dansylamide and enzyme mixture was prepared. Aliquots of 100 µl of the dansylamide and enzyme mixture were dispensed into each well using a multi-

channel pipette, giving final concentrations of 20 μM dansylamide and 1 μM CA II per well. 1 μl aliquots of inhibitor were dispensed from the dilution source plates into the 96-well fluorescent plates (Costar) containing CA II and dansylamide using a 96-channel programmable liquid handling workstation (Plate Trak, CCS Packard, Torrence CA). The reaction mixture was allowed to equilibrate at room temperature for 20 minutes with gentle stirring. The fluorescence spectra were then recorded using a Fluostar fluorimeter (BMG Labtechnologies, Germany), with excitation wavelength set at 280 nm and emission wavelength set at 470 nm.

A gain setting of 115 was applied. This was done to allow for optimal signal: noise ratio and was achieved by using the wells with expected maximum fluorescence (negative control wells) to calibrate the fluorimeter. The inhibitor binding constants and error estimates were determined with the Graphpad Prism curve-fitting program (Version 4.0) using equation 4 below.[64]

$$\text{fraction } F_{total} = \frac{F_{obs} - F_{end}}{F_{ini} - F_{end}} = \frac{1}{1 + (K_{DNSA}/[DNSA])(1 + [I]/K_I)} \qquad (4)$$

F_{total} represents the total fluorescence

F_{obs} represents the observed fluorescence (fluorescence observed in a well with a given dansylamide concentration)

F_{ini} represents the initial fluorescence of the protein devoid of dansylamide binding (minimum fluorescence)

F_{end} represents the fluorescence end point (maximum fluorescence)

K_{DNSA} represents the dansylamide dissociation constant

[DNSA] represents the dansylamide concentration in a plate well

K_I represents the inhibitor dissociation constant

2.5 Ellman's Reagent Test

The sulfhydryl content of certain tissues was observed to have changed as a result of drug action. This observation led George Ellman in 1959 to devise a method for measurement of protein sulfhydryls.[65] In this spectrophotometric method, 5, 5'-dithio-bis (2-nitrobenzoic acid) (DTNB), also known as Ellman's reagent, is used. This experiment is based on the reaction the thiolate anion ($R\text{-}S^-$) with Ellman's reagent ($DTNB^{2-}$). This results in a mixed disulfide product ($R\text{-}S\text{-}TNB^-$) and TNB^{2-} (5-thio-2-nitrobenzoic acid) (Figure 11).

The TNB^{2-} produced exhibits an intense molar absorption at 412 nm. This absorption relates to only one of the species in solution as the other two species, $DTNB^{2-}$ and $R\text{-}S\text{-}TNB^-$ exhibit only a weak absorption at 412 nm. Factors affecting the performance of this assay have been evaluated but overall it is a rapid and simple spectrophotometric assay for thiol quantitation.[66] For some heteroatomic cyclic organic molecules such as thiosugars, the rates of ring-opening and closing and proportion of sugar with free SH groups have been studied using DTNB among other reagents.[67] This suggests that DTNB can be used to study the hydrolysis of thioxolone if it resulted in the formation of a thiol group.

Based on the preliminary X-ray crystallography study, the hydrolysis of thioxolone would result in an aromatic molecule with a free SH group (Figure. 5,

McKenna, Personal communication). To obtain further proof of this possibility, DTNB was added to a reaction mixture containing increasing amounts of thioxolone and a limiting amount of CA II and the rate of absorption at 412 nm measured. A DTNB stock solution was prepared containing 2 mM DTNB and 50 mM sodium acetate. The reaction was carried out in 50 mM MOPS buffer, pH 7.5. The total sample volume was made up to 1 ml with DI water and the reagents were added to a quartz cuvette with a 1cm path length. The final concentrations were 100 μM DTNB, 200 nM CA II and two concentrations of 500 μM and 1 mM thioxolone were used. A stock enzyme solution of 10 μM was used.

The volumes of reagents were added as follows to give a 1 ml total volume:

Table 4

Volumes of Reagents

Sample	DTNB	MOPS	CA II	DI Water	Thioxolone
1	50 μl	100 μl	20 μl	830 μl	0 μl
2	50 μl	100 μl	0 μl	800 μl	50 μl
3	50 μl	100 μl	0 μl	750 μl	100 μl
4	50 μl	100 μl	20 μl	780 μl	50 μl
5	50 μl	100 μl	20 μl	730 μl	100 μl

The reagents were carefully mixed in the cuvette using a pipette and the absorbance monitored at 412 nm using a Spectramax spectrophotometer (Molecular Devices) for 4 minutes. The readings were taken both in the presence and absence of

thioxolone and the results were compared. The effect of increasing the concentration of thioxolone was also studied.

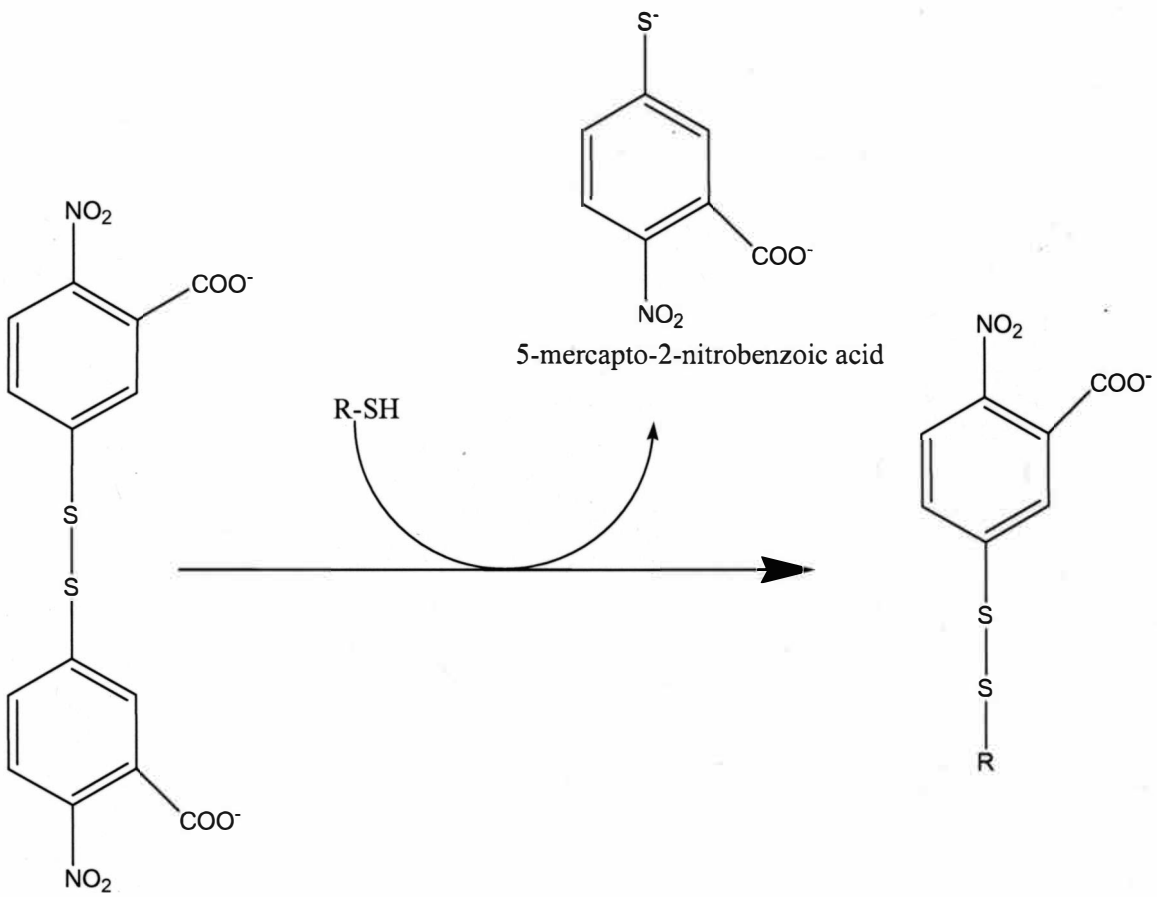

Figure 11. Reaction of Ellman's reagent with a thiol

2.6 Inhibition Kinetics of CA II by Thioxolone

CA II inhibitors have been reported that belong to the three main classes of inhibitors namely competitive, noncompetitive (mixed) and uncompetitive. Anions inhibit CA esterase activity in a non-competitive manner and this group of anions includes fluoride, chloride, acetate, bromide, nitrate, iodide and thiocyanate.[12]

Imidazole and phenol have been reported to be competitive inhibitors of CA I and II respectively. These competitive inhibitors act on the CO_2 hydrase activity. [3; 50]

Uncompetitive inhibitors have been reported and the dianion sulfate is an example.[49] The mode of inhibition by thioxolone has not been reported and in this study, an investigation was carried out using classical Michealis-Menten [68] enzyme kinetics parameters to elucidate the inhibition pattern. The parameters studied include K_M, defined as the substrate concentration required to give half maximal velocity and V_{max}, defined as the maximum reaction rate for a given enzyme concentration, as given in equation 4, below .

These parameters are dependent on the type of inhibition and when measured in the presence and absence of inhibitor, they can aid in the determination of the type of inhibition.

$$V_o = \frac{V_{max}[S]}{K_M + [S]} \quad (4)$$

Michealis-Menten equation

Competitive inhibitors compete with substrate for the enzyme binding site. This results in a reduction of the free enzyme that can catalyze the reaction. However, high substrate concentrations can reduce and remove the effects of competitive inhibition. Competitive inhibitors act to increase $K_M\left(K_M^{app}\right)$. [68]

$$V_o = \frac{V_{max}[S]}{\alpha K_M + [S]} \qquad \text{where} \quad \alpha = \left(1 + \frac{[I]}{K_I}\right) \quad (5)$$

Michealis-Menten equation for competitive inhibition.

Uncompetitive inhibitors bind the enzyme-substrate complex preventing catalysis. They achieve this by distorting the enzyme active site thereby rendering it catalytically inactive. Uncompetitive inhibitors have no effect on substrate affinity and increased substrate concentrations do not abolish the effects of uncompetitive inhibition on V_{max}.[68]

$$V_o = \frac{V_{max}[S]}{K_M + \alpha'[S]} \quad \text{where} \quad \alpha' = \left(1 + \frac{[I]}{K_I'}\right) \quad (6)$$

Michealis-Menten equation for uncompetitive inhibition

Mixed (noncompetitive) inhibitors show characteristics of both competitive and uncompetitive inhibition. Consequently, both the enzyme and enzyme-substrate complex bind the inhibitor. The net effect is that K_M is increased and V_{max} is reduced.[68]

$$V_o = \frac{V_{max}[S]}{\alpha K_M + \alpha'[S]} \quad \text{where } \alpha = \left(1 + \frac{[I]}{K_I}\right) \text{ and } \alpha' = \left(1 + \frac{[I]}{K_I'}\right) \quad (7)$$

Michealis-Menten equation for mixed inhibition

Measuring the initial velocity (V_o) rates at different substrate and inhibitor concentrations allows the net effects of the inhibitor on the parameters V_{max} and K_M to be determined and the type of inhibition determined. In this study, the effect of thioxolone on the CA II esterase activity was studied using 4-nitrophenyl acetate as the substrate and the effects on the Michealis-Menten parameters evaluated.

The Michealis-Menten parameters K_M and V_{max} were determined both in the absence and in the presence of two different inhibitor concentrations. The substrate

used was *p*-nitrophenyl acetate and the concentration was varied between 125 μM and 1.95 μM. A CA II concentration of 1 μM was used for all the samples. The thioxolone concentrations used were 50 μM and 500 μM respectively for those samples that included the inhibitor.

To achieve the desired series of *p*-nitrophenyl acetate concentrations (*p*-NPA), a 125 μM stock solution of *p*-NPA was prepared in DMSO. A consecutive series of 1:2 dilutions was then carried out resulting in concentrations of 125, 62.5, 31.25, 15.63, 7.81, 3.91 and 1.95 μM respectively. The total volume in the reaction mixture was maintained constant at 1.0 ml as were the quantities of each reagent added. The volume was made up to 1ml by addition of 50 mM MOPS buffer, pH 7.5.

The initial rates were first determined in the absence of inhibitor and volumes of reagent added and concentrations were as follows:

Table 5

Volumes and Concentrations of Reagents

Sample	CA II (μl)	4-NPA (μl)	MOPS buffer (μl)	CA II (μM)	4-NPA (μM)
1	20.0	50.0	930.0	1.0	125.0
2	20.0	50.0	930.0	1.0	62.50
3	20.0	50.0	930.0	1.0	31.25
4	20.0	50.0	930.0	1.0	15.63
5	20.0	50.0	930.0	1.0	7.81
6	20.0	50.0	930.0	1.0	3.90
7	20.0	50.0	930.0	1.0	1.95

The reagents were added to a quartz cuvette with a 1 cm. path length in the following order: MOPS buffer, CA II and *p*-nitrophenyl acetate was added last. The reaction mixture was mixed using a pipette and the absorbance read at 348 nm,

following the liberation of the nitrophenolate anion upon *p*-nitrophenyl acetate hydrolysis. Absorbance measurements were taken using a Spectramax spectrophotometer interfaced with an IBM-compatible computer.

Data points were collected every 30 seconds for 3 minutes and the initial rate was recorded as change in optical density per minute. The raw data was analyzed using Softmax Pro (Version 4.7) analysis software. The data was fitted using Graphpad Prism (Version 4.0) software applying standard Michealis-Menten kinetics. The effects of thioxolone inhibition on carbonic anhydrase were investigated by preparing the samples as described above but with addition of 50 μM and 500 μM thioxolone to the reaction mixture to give the following total volumes:

Table 6

Volumes of Reagents

Sample	CA II	*p*-NPA	MOPS buffer	Thioxolone
1	20.0 μl	50.0 μl	880.0 μl	50.0 μl
2	20.0 μl	50.0 μl	880.0 μl	50.0 μl
3	20.0 μl	50.0 μl	880.0 μl	50.0 μl
4	20.0 μl	50.0 μl	880.0 μl	50.0 μl
5	20.0 μl	50.0 μl	880.0 μl	50.0 μl
6	20.0 μl	50.0 μl	880.0 μl	50.0 μl
7	20.0 μl	50.0 μl	880.0 μl	50.0 μl

The reagents were added to a quartz cuvette with a 1 cm. path length in the following order: MOPS buffer, CA II, thioxolone and *p*-NPA was added last. The reaction mixture was mixed using a pipette and the absorbance read at 348 nm, following the liberation of the nitrophenolate anion upon *p*-NPA hydrolysis. Absorbance measurements were taken using a Spectramax spectrophotometer

(Molecular Devices) interfaced with an IBM-compatible computer. Data points were collected every 30 seconds for 3 minutes and the initial rate was recorded as change in optical density per minute. The raw data was analyzed using Softmax Pro (Version 4.7) analysis software. The data was fitted using Graphpad Prism (Version 4.0) software applying Lineweaver-Burk kinetics and the parameters K_M and V_{max} determined.

2.7 Nuclear Magnetic Resonance and Infrared Spectroscopy

NMR studies and IR were carried out on pure thioxolone and an extract of the enzyme-thioxolone reaction mixture. The method used to extract the reaction mixture was by Wessel and Flugge [69] employing methanol-chloroform extraction. The thioxolone samples were of the pure compound from Sigma Aldrich. The IR samples were prepared using potassium bromide (KBr) to form a disc which was mounted on a Fourier-Transform Infrared Spectrophotometer (FTIR) (Perkin Elmer 1710) and the spectrum recorded.The NMR samples were dissolved in deuterated DMSO and spectra recorded on a 400 MHZ multinuclear NMR spectrophotometer (Jeol JNM-ECP400).

2.8 Liquid Chromatography-Mass Spectroscopy Studies

LC-MS studies were carried out on thioxolone and a sample of the reaction mixture. The samples were prepared in methanol. The thioxolone sample was

prepared by dissolving 0.1 mg thioxolone in 1 ml of methanol. The sample of the reaction mixture was a result of chloroform-methanol extraction using the method of Wessel and Flugge [69] that resulted in the precipitation of CA II from an incubation mixture of CA II and thioxolone. The supernatant was collected and dried under a vacuum in a dessicator and reconstituted in methanol. The samples were manually injected in an LC-MS (Shimadzu LC-MS 2010) and ionized in the negative mode and the spectra recorded.

2.9 Hydrolysis Studies Using UV-VIS Spectroscopy

The hydrolysis of thioxolone in the presence of CA II was studied by comparing thioxolone hydrolysis in the presence and absence of CA II. Thioxolone is an ester and it hydrolyzes in solution. However, the proportion of thioxolone hydrolyzed would be expected to be higher in the presence of CA II and this would be suggestive of the possibility of thioxolone cleavage by CA II.

A 10 μM sample of thioxolone in 50 mM MOPS buffer was dispensed into a quartz cuvette with a 1 cm. path length. Another sample containing mixture of 1 μM CA II and 10 micromolar thioxolone in 50 mM MOPS buffer was dispensed into a quartz cuvette with a 1 cm.path length. The total sample volume was maintained at 1 ml. Spectra were taken at a 1 hour interval and the spectra were recorded on a diode-array spectrophotometer (Hewlett Packard, HP 8452A) set to collect wavelengths between 190 nm and 510 nm.

CHAPTER III

RESULTS

3.1 Inhibition of Carbonic Anhydrase II: Specs Compounds

Inhibition of CA II was determined for thioxolone and its analogs (Figure 7) using the esterase method reported [12] and inhibitory activity computed as IC_{50} values. The results are reported in Table 7 below. Raw data is presented in appendix A.

Table 7

IC_{50} Values for CA II Inhibitors as Determined by the Esterase Method

Compound	IC_{50} value (M), x 10^{-6}
Thioxolone	9.39 ± 0.530
Acetazolamide	0.444 ± 0.020
Methazolamide	0.293 ± 0.044
2-Mercaptophenol	1.05 ± 0.005
Benzenethiol	1.49 ± 0.11
Specs 1	5.69 ± 1.64
Specs 2	No inhibition
Specs 3	No inhibition
Specs 4	5.95 ± 0.726
Specs 5	0.841 ± 0.176
Specs 6	0.867 ± 0.061
Specs 7	0.912 ± 0.054
Specs 8	0.842 ± 0.187
Specs 9	0.728 ± 0.223
Specs 10	0.324 ± 0.037
Specs 11	0.526 ± 0.023
Specs 12	No inhibition
Specs 13	1.89 ± 0.331
Standard Errors reported for IC_{50} values fitted in appendix A	

Three compounds were non-inhibitory and these were compounds 2, 3 and 12. The inhibitory species that were more potent than thioxolone were acetazolamide,

methazolamide, 2-mercaptophenol, benzenethiol, specs 1, specs 4, specs 5, specs 6, specs 7, specs 8, specs 9, specs 10, specs 11 and specs 13.

3.2 Analogs from Dr. James Kiddle and Wright state University

Three compounds (Figure 8) synthesized by Dr. James Kiddle at Western Michigan University were also assayed for CA II inhibition activity using the esterase method and found to be inhibitory. Compounds 1 and 2 had IC_{50} values that were lower than for thioxolone while compound 3 was less potent than thioxolone. The results are tabulated below in Table 8. Raw data is presented in appendix A.

Table 8

IC_{50} Values of Thioxolone Analogs from Dr. James Kiddle

Compound	IC_{50} value, x 10^{-6} M
1	1.16 ± 0.115
2	0.969 ± 0.169
3	17.9 ± 5.09

Standard Errors reported for Log IC_{50} fitted in appendix A

A total of 19 sulfonamides compounds and synthetic precursors were provided courtesy of Dr. Daniel Ketcha of Wright State University (Figure 9). Only six of these were found to be inhibitory as assayed by the esterase method. These compounds were compound 008, compound 009, compound 010, compound 011, compound 012 and compound 015. The IC_{50} results are shown in Table 9. Raw data is available in appendix A.

Table 9

IC_{50} Values of Inhibitory Sulfonamides from Wright State University

Compound	IC_{50} value (M) x 10^{-6}
WSU-DMK 008	29.5 ± 3.18
WSU-DMK 009	16.3 ± 0.703
WSU-DMK 010	18.9 ± 1.12
WSU-DMK 011	28.7 ± 4.93
WSU-DMK 012	10.4 ± 0.680
WSU-DMK 015	51.4 ± 12.5
Standard Errors reported for IC_{50} fitted in appendix A	

3.3 Inhibitor Binding Studies

Inhibitor binding studies were carried out on the inhibitory specs compounds. This was based on a competitive binding assay with dansylamide and this required the establishment of the binding affinity of dansylamide to CA II first. The dissociation constants of the inhibitors to CA II were then determined relative to that of dansylamide. The dissociation constants were determined for dansylamide, thioxolone, acetazolamide, methazolamide, 2-mercaptophenol, benzenethiol, specs 1, specs 2, specs 3, specs 4, specs 5, specs 6, specs 7, specs 8, specs 9, specs 10, specs 11,specs 12 and specs 13. The results are shown below in Table 10.

Table 10

CA II Inhibitor Dissociation Constants

Compound	Dissociation Constant value (K_d, M) x 10^{-6}
Dansylamide	2.91 ± 0.098
Thioxolone	6.21 ± 1.65
Acetazolamide	0.012 ± 0.002
Methazolamide	0.047 ± 0.006
2-Mercaptophenol	0.769 ± 0.073
Benzenethiol	0.741 ± 0.092
Specs 1	2.49 ± 0.296
Specs 2	0.357 ± 0.112
Specs 3	4.55 ± 0.461
Specs 4	2.79 ± 0.454
Specs 5	2.98 ± 0.499
Specs 6	0.337 ± 0.041
Specs 7	4.86 ± 0.754
Specs 8	7.97 ± 2.39
Specs 9	1.38 ± 0.151
Specs 10	11.7 ± 1.26
Specs 11	0.564 ± 0.047
Specs 12	4.61 ± 1.02
Specs 13	7.43 ± 0.666

Standard Errors reported for K_D values fitted in appendix B

The binding assay exploited the enhanced fluorescence of dansylamide when bound to enzyme active sites and its diminished fluorescence when an inhibitor binds thereby displacing it. The effects of CA II and inhibitor binding on dansylamide fluorescence are shown in Figure 12. Dansylamide fluorescence is enhanced upon addition of CA II due to binding of dansylamide and diminishes upon addition of thioxolone due to inhibition of dansylamide binding.

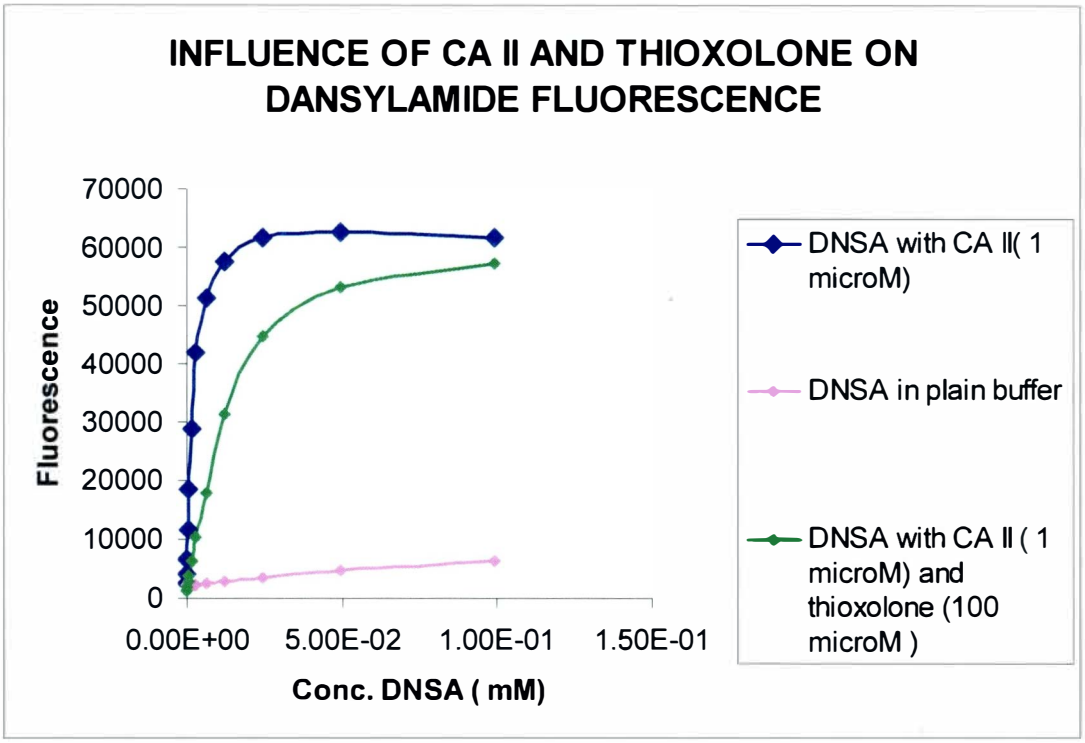

Figure 12. Effect of CA II and inhibitor on dansylamide fluorescence.

3.4 Ellman's Reagent Test

Ellman's reagent forms mixed disulfides with thiols and has also be used to study ring opening and closing rates for thiosugars.[67] In this research study, it was used to study the effect of CA II on thioxolone hydrolysis and the results are shown in Figure 13 below. There is an increase in absorbance at 412 nm with increasing amounts of thioxolone and a limiting amount of CA II. This is suggestive of increased free thiol groups due to the formation of 5-mercapto-2-nitrobenzoic acid probably arising from thioxolone cleavage by CA II. This implies that CA II cleaves thioxolone upon binding.

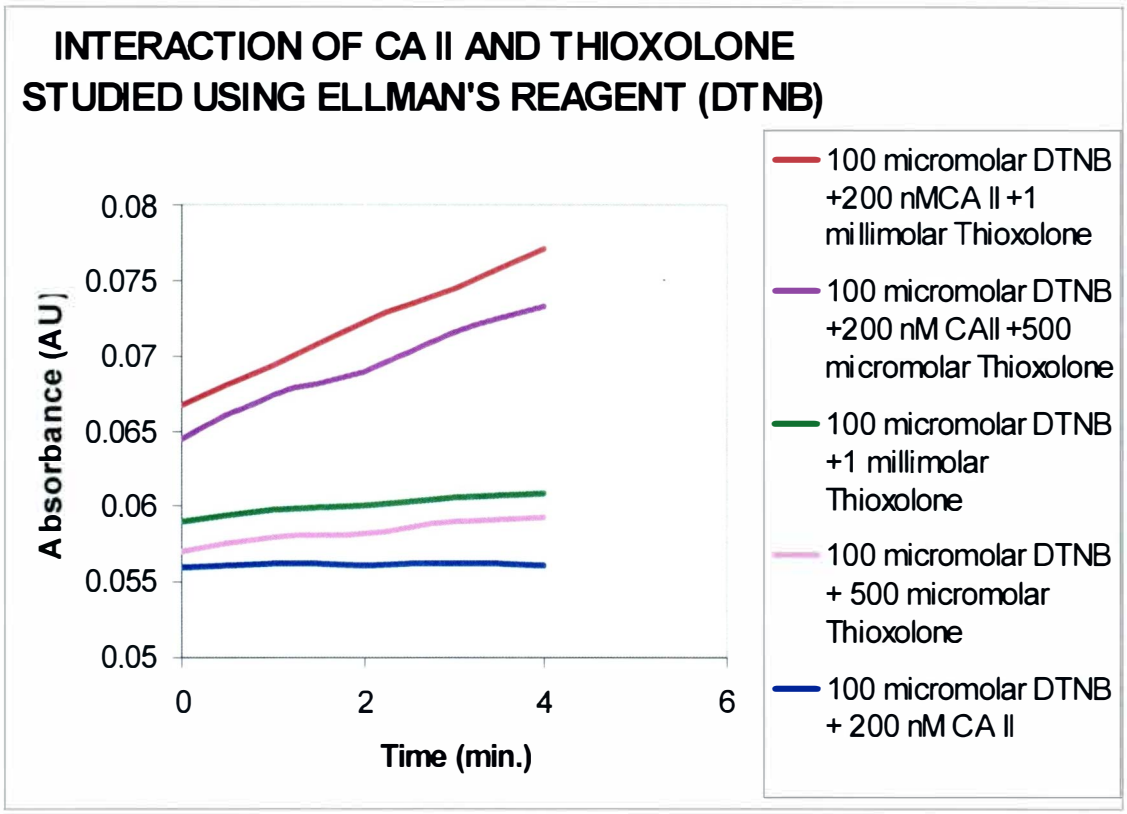

Figure 13. Reaction of thioxolone and Ellman's reagent (DTNB) in the presence of CA II.

3.5 Michealis-Menten Kinetics Results

Kinetics studies were carried out on CA II both in the absence of and in the presence thioxolone. The substrate for this study was *p*-nitrophenyl acetate and different concentrations were used. CA II concentration was 1 μM the thioxolone concentrations used were 50 and 500 μM. There was a decrease in initial reaction velocity with increasing thioxolone concentration. The substrate-velocity graphs are shown below.

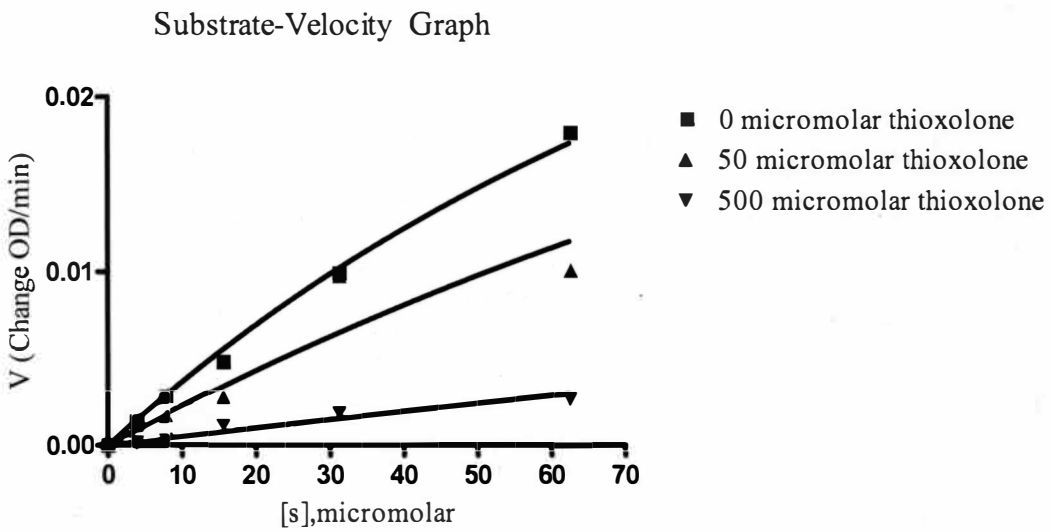

Figure 14. Substrate-velocity graphs of CA II in the presence of thioxolone.

In addition, Lineweaver-Burk plots were fit to this data in order to determine the Michealis-Menten parameters V_{max} and K_M. There was a decrease in V_{max} and an increase in K_M, both characteristics of mixed inhibition suggesting that thioxolone acts as a mixed inhibitor of CA II. The Lineweaver-Burk plot is shown in figure 15 and supports the conclusion that thioxolone is a mixed inhibitor.

3.6 Infrared Spectroscopy

Potassium bromide (KBr) discs of thioxolone and the solid extract from the reaction mixture were prepared and IR analysis performed on a Fourier-Transform Infrared Spectrophotometer (FTIR) (Perkin Elmer 1710). The IR spectrum of thioxolone reveals the presence of a benzene ring (>3000 cm^{-1}) and the carbonyl group (1750 cm^{-1}) (Appendix B).

Lineweaver-Burk of Nonlin fit of Substrate-velocity data

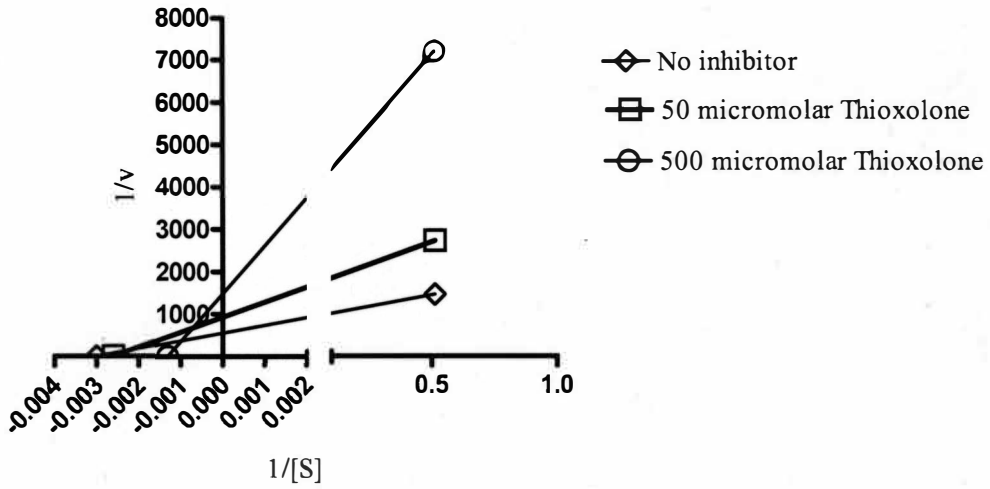

Figure 15.Lineweaver-Burk plots of increasing thioxolone concentration.

The peak positions for other thioxolone functional groups are as follows: phenolic hydroxyl (3355 cm^{-1}), C-C-O stretch (1220 cm^{-1}), C-S stretch (700 cm^{-1}) (Appendix C). The IR of the thioxolone hydrolysis product does not exhibit the presence of an aromatic ring. There are no C-H peaks above 3000 cm^{-1} hence no aromatic ring on the product.

3.7 Nuclear Magnetic Resonance Spectroscopy

NMR samples of thioxolone and the reaction mixture extract were prepared in deuterated DMSO. The proton NMR spectrum of thioxolone has the hydroxyl resonance at a chemical shift of 10 ppm (Appendix D). The aromatic ring protons exhibit chemical shift at 6.7-7.6 ppm. The C1 proton has a chemical shift of 7.5 ppm (doublet) and the C4 proton has a shift of 6.8 ppm (doublet). The C5 proton has a chemical shift of 6.7 ppm (doublet of doublet).

The thioxolone hydrolysis product exhibits no resonance in the aromatic range for protons. The spectrum has a strong residual HOD signal (3.3 ppm) and the DMSO (2.5 ppm) solvent peak is prominent. There are additional peaks at 1.7 and 1.3 ppm and these could be attributed to the carboxylic acid hydroxyl group resulting from thioxolone hydrolysis.

3.8 Liquid Chromatography-Mass Spectroscopy

A solid sample of the reaction mixture from chloroform-methanol extraction was reconstituted in methanol. A thioxolone sample was also dissolved in methanol and both samples were analyzed using LC-MS. The LC-MS analysis method applied negative ionization mode due to the fact that thioxolone has a hydroxyl group that readily loses a proton. A trial run was made with thioxolone to determine which mode of ionization would yield the expected *m/z* ratio for thioxolone.

The negative ionization mode resulted in the deprotonated ion $[M-H]^-$ at *m/z* 167 (Appendix E). Another peak was observed at *m/z* 335 suggesting the formation of dimers by thioxolone. This was probably a result of formation of disulfide bonds between two thioxolone molecules. Another sample of the derivative 2-mercaptophenol was also run in the negative ionization mode. The deprotonated ion peak $[M-H]^-$ was observed at m/z 125.

Other peaks were observed at m/z 249 *and m/z* 373. These correspond to the formation of a dimer and a trimer respectively. Investigation of the reaction mixture

sample resulted in a peak at *m/z* 208. Upon running a sample with plain buffer, the source of this peak at *m/z* 208 was found to be the MOPS buffer.

3.9 Thioxolone Hydrolysis in the Presence and Absence of CA II

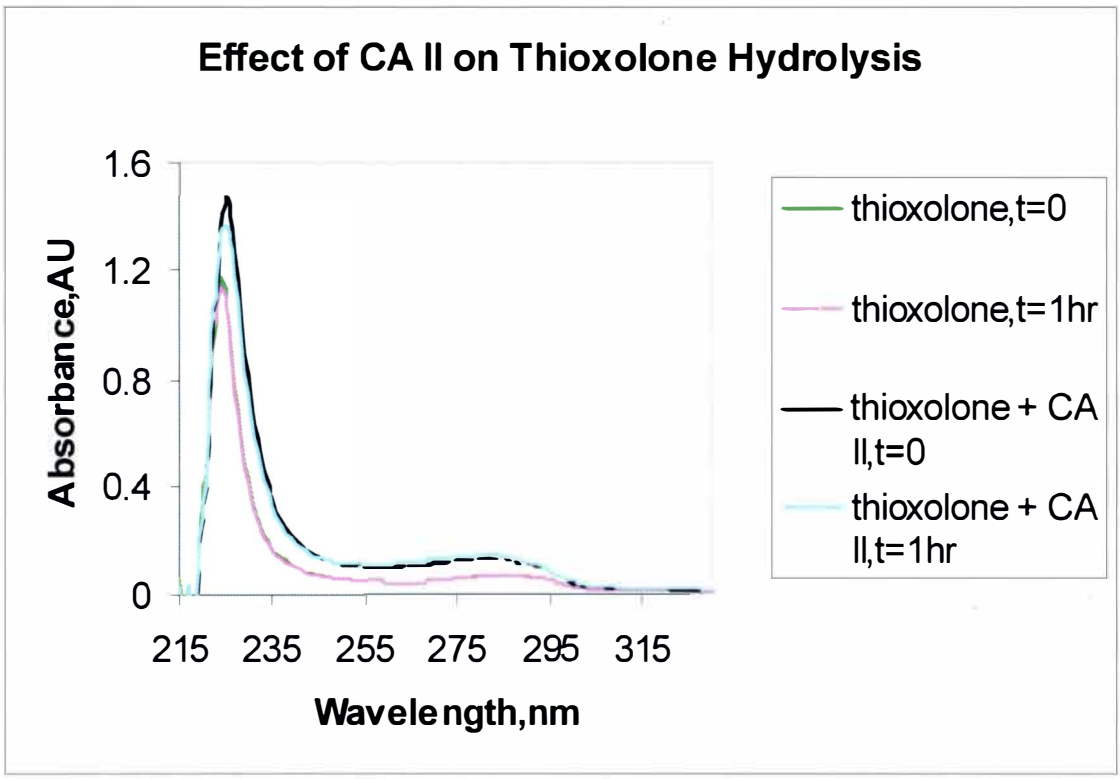

Figure 16. Effect of CA II on thioxolone hydrolysis.

A sample containing 10 μM thioxolone was prepared in buffer of pH 7.5 containing 50 mM MOPS, 33 mM Na_2SO_4 and 33 mM EDTA. Another sample containing 10 μM thioxolone and 1 μM CA II was prepared in a buffer of similar composition. Thioxolone hydrolysis was expected to be higher in the presence of CA II leading to a decrease in the absorption peak.

Initial UV-visible spectra were collected for both samples using a diode-array spectrophotometer. Spectra were taken again after 1 hour and thioxolone hydrolysis found to be higher in the sample containing CA II (Figure 16). This implies that in addition to thioxolone hydrolysis in solution, CA II also hydrolyzes thioxolone hence the hydrolysis observed in the presence of CA II is higher than that observed in its absence.

CHAPTER IV

DISCUSSION AND CONCLUSIONS

4.1 Inhibition of Carbonic Anhydrase II: Specs Compounds

Inhibition of CA II was determined using the esterase method reported [12] and inhibitory activity by acetazolamide, a benchmark sulfonamide inhibitor, determined. The IC_{50} value determined for acetazolamide was 0.444 μM (Table7). The inhibition activity of thioxolone and its analogs was also determined by this assay and the results were recorded (Table7). The results indicate that thioxolone is a weak inhibitor of CA II compared to the sulfonamides acetazolamide and methazolamide.

Thioxolone exhibits weak CA II esterase activity inhibition with an IC_{50} value of 9.39 μM (Table7). The sulfonamides acetazolamide and methazolamide have IC_{50} of 0.444 and 0.293 μM respectively. However, one of the thioxolone analogs exhibited an IC_{50} value comparable to the sulfonamides acetazolamide and methazolamide. Specs compound 10 resulted in an IC_{50} value of 0.324 μM suggesting that its CA II inhibitory potency was comparable to that of methazolamide and acetazolamide.

It differs from thioxolone in that it has an extra ester side chain with an aromatic ring. These may improve its hydrogen bonding ability and hydrophobic interactions with the hydrophobic pocket. Its basic structure, being a derivative of thioxolone, indicates that changes can be made on the thioxolone structure to enhance CA II inhibitory potency.

Other compounds with IC_{50} values lower than thioxolone include compounds 5, 6, 7, 8, 9, 10 and 11 (Table 7). The main variations to the basic thioxolone structure included addition of straight-chain substituents and aromatic rings. Interestingly, both changes led to an increase in inhibition activity. This illustrates the CA II active site's ability to accommodate a wide range of structural variations to the thioxolone molecule. This allows for wider variation in structure while maintaining the inhibitory potency that is a highly desirable feature for a template around which drugs can be designed.

Another structural modification of thioxolone employed in these analogs is halogenation. The effect of halogenation on CA II inhibition was found to have varying effects on the inhibitory potency. Of this entire series of analogs, those that did not exhibit inhibition were halogenated. Compounds 2 and 3 (Figures 7) were brominated on two positions of the benzene ring. Compound 12 (Figure 7) was chlorinated on two positions of a benzene ring substituent. This can be related to the extent of halogenation and the position of the halogen atoms since less halogenated compounds were more potent. Compounds 6, 7 and 8 (Figures 7) are monobrominated and have improved inhibition compared to thioxolone.

Compound 9 is also chlorinated at two positions but has inhibitory potency in the sub-micromolar range (0.728 μM). The difference in potency can thus be attributed to the differences in structure, type and positioning of the substituents. Bromine is a relatively bulky atom and may confer steric hindrance at the CA II active site. The degree of steric hindrance is bound to increase as the number of bromine

atoms on the inhibitor molecule increases and this may explain why compounds 2 and 3 are non-inhibitory. However, the trifluorinated specs compound 11, which is the most halogenated compound in the series, is highly inhibitory with an IC_{50} of 0.526 micromolar (Table 7). Fluorine is a smaller atom relative to bromine and could thus be more efficiently packed into the CA II active site without resulting in steric hindrance. This illustrates how slight structural modifications can lead to large changes in activity.

Two molecules, 2-mercaptophenol and benzenethiol, that are devoid of the extended ring structure show moderate inhibition of CA II. This indicates that the part of the extended ring oxathiolone structure may not be very vital for inhibitory potency. These molecules possess an aromatic ring that can lead to favorable hydrophobic interactions with the hydrophobic pocket of the active site. In addition, they possess possible binding groups: a thiol and a hydroxyl group for 2-mercaptophenol and a thiol group for benzenethiol.

Hydrogen bond networks are important at the CA II active site [45] and therefore functional groups that favor these interactions are likely to be a good fit for the active site. The zinc-bound hydroxide group at the CA II active site donates a hydrogen bond to a threonine-199 residue and this aids in orientation of the hydroxide group for nucleophilic attack [7]. This importance of hydrogen bond networks may be responsible for the trends observed in these inhibitors. Inhibitors with hydrogen bond acceptors as side chains exhibited better inhibition with lower IC_{50} values compared to those

without hydrogen bond acceptors. Esters are hydrogen bond acceptors and the inhibitors 5, 7, 8,9,10 and 11 were all esters (Figure 7).

The addition of hydrogen bond acceptors can therefore be seen as beneficial to thioxolone analogs with regard to CA II inhibition. The CA II active site is situated in a hydrophobic pocket [7] and binding to these pocket involves hydrophobic interactions. Groups favoring hydrophobic interactions include aromatic rings and their inclusion into the side chains of inhibitors has been shown to improve CA inhibition over that by thioxolone. The inhibitors 5,8,9,10,11 and13 have lower IC_{50} values compared to thioxolone (Table 7). These also have an oxygen atom ester linkage which can act as a hydrogen bond acceptor improving interactions with the active site while the aromatic ring improves interactions with the hydrophobic pocket of the active site.

4.2 Inhibitor Binding Studies

The CA II active site contains one catalytic zinc ion enveloped in a hydrophobic pocket. This hydrophobic pocket consists of the amino acids leucine-198, valine-143 and valine-121 [7]. At the active site, the metal ion is coordinated directly to three histidine residues (His-94, His-96, His-119) and a water molecule in tetrahedral fashion. Another group of indirect ligands (Gln-92, Glu-117, Asn-244) form hydrogen bonds with the directly coordinating histidine residues and a Thr-199 residue accepts a hydrogen bond from the zinc-bound hydroxide.

The β-strand containing the direct histidine ligands is anchored in the hydrophobic shell of the enzyme by the aromatic residues Phe-93, Phe-95, and Trp-97. [70] Inhibition of CA II involves coordination of the inhibitor molecule to the catalytic metal ion. Consequently, an inhibitor molecule must contain a zinc-binding moiety as part of its structure. Sulfonamide drugs that act as CA II inhibitors owe this to the sulfonamide group that has been found to be a very good zinc-binding group. Additionally, most CA II inhibitors incorporate aromatic or heteroaromatic functional groups to enhance favorable interactions with the hydrophobic region of the active site.

In this study, the CA II dissociation constants were determined for thioxolone and its analogs and these were compared to those of the benchmark sulfonamide CA II inhibitors acetazolamide and methazolamide. The dissociation constants were determined based on the competitive binding assay with dansylamide reported.[64] The dissociation constants determined for the benchmark sulfonamide inhibitors acetazolamide and methazolamide were indicative of the tight binding characteristic of sulfonamides on CA II (Table 10). Thioxolone, on the other hand, binds weakly to CA II compared to the sulfonamides. The dissociation constant for thioxolone was about 500 times greater than that of acetazolamide. This may account for the relatively lower inhibition activity observed.

The thioxolone analogs resulted in varying magnitudes of CA II binding affinity. Improvement in CA II binding affinity over thioxolone was observed in specs compounds 1, 2, 3, 4, 5, 6, 7, 9, 11 and 12 (Table 8). The main structural

modifications made on thioxolone were addition of aromatic or aliphatic side chains and halogenation. Aromatic side chains favor hydrophobic interactions between the inhibitor molecule and the non-polar amino acids valine and leucine lining the hydrophobic pocket [7]. Hydrophobicity may act to reduce the dielectric constant at the active site. Stronger ligand-metal electrostatic interactions are expected in an environment with low dielectric constant. [71] This may account for the improved affinity by specs compounds 5, 9, 11 and 12 (Table 8).

Specs compounds 1 and 4 have non-polar sides that can also actively interact with the hydrophobic pocket amino acids. Specs compound 1 has a straight-chain hydrocarbon side group and specs compound 4 has a cyclic hydrocarbon chain. Compounds with ester side chains resulted in higher binding affinity and this could be as previously mentioned, a consequence of the property of esters as hydrogen bond acceptors.

Halogenated sulfonamide CA inhibitors have been reported to be more potent than their non-halogenated counterparts.[35; 38; 53] Specs Compound 6 bears very close similarity with thioxolone with the only difference being the bromine atom attached on the C5 carbon atom of the benzene ring. However, it appeared to bind to CA II with a higher affinity than thioxolone. Bromine is a relatively large atom and may confer steric hindrance at the active site, especially if more than one atom is attached to an inhibitor molecule. However, when only one atom is attached to the inhibitor structure, as observed in specs compounds 6 and 7, it appears to make a remarkable contribution towards the improvement of the affinity of the enzyme active site to the

inhibitor. The bromine atom in specs compound 6 may lead to polarization of the phenolic hydroxyl group (Figure 7) making it a better hydrogen bond donor to acceptor groups in amino acids at the active site.

Some inhibitors were structurally similar yet a slight change in the structure led to very different dissociation constant values. Specs compounds 10 and 11 only differ structurally in one position. At the C4 carbon atom of the benzene ring, compound 10 has a nitro- group attached while compound 11 has a trifluoro- group attached at position 3. However, the affinity of CA II is greater for compound 11 than it is compared to compound 10. This can be attributed to the electronegativity of the fluorine atoms that may lead to the lowering of the pK_a of the –SH group formed upon hydrolysis of the original compound resulting in bond formation between the sulfur atom and the active site zinc atom. The electron-withdrawing effects may also lead to a shortening of the bond between the sulfur and the zinc atoms.

The CA II active site is situated in a hydrophobic pocket and this has directed the design of CA II inhibitors to include aryl- and heteroaryl groups for favorable interactions with the active site. The inclusion of aromatic rings in the inhibitor structure increases hydrophobic interactions between the inhibitor and the active site. Compounds 1 and 3 have aliphatic side chains attached to the thioxolone structure and these are capable of forming hydrophobic interactions with the highly hydrophobic pocket of the active site. This may be the major contributing factor to the low dissociation constant values observed for these compounds. The side chain of

compound 3 is more polar than that of compound 1 and therefore may not interact as well with the hydrophobic pocket resulting in a slightly higher dissociation constant.

The two thioxolone derivatives, 2-mercaptophenol and benzenethiol, exhibit tight binding in the nanomolar range. Benzenethiol has a sulfur atom that can function as a zinc ion-binding group and this shows that the sulfur atom in thioxolone hydrolysis product can act as a zinc-binding moiety. 2-mercaptophenol also has a thiol group in addition to a hydroxyl group and given the close similarity in dissociation constants between these two inhibitor molecules, they may bind to CA II via the same group, the thiol group.

These two molecules resemble the possible hydrolysis products of thioxolone and lack the multiple aromatic ring systems. This is an example of how adept the CA II active site can be at accommodating a diverse range of molecules. Potent straight-chain CA II inhibitors have been reported [36] and this shows that the aromatic ring may not necessarily be required for all types of CA II inhibitors.

A low dissociation constant implies tighter binding and should therefore result in low IC_{50} values implying more potency. However, in some instances low dissociation constants did not correlate with low IC_{50} values. This may be as a result of inhibitor binding to a different site rather than the actual catalytic site. During preliminary x-ray crystallographic studies, evidence reported the possible existence of more than one thioxolone hydrolysis product binding site in the CA II active site. Binding to more than one site can account for the discrepancies in IC_{50} values that did not correlate with dissociation constants as expected.

The discrepancies between inhibitor binding and potency can be accounted for by allosteric regulation of CA II. The possibility of more than one binding site on the CA II active site supports the fact that molecules may bind at one position and induce a conformational change influencing the binding properties of the active site at another position. This will imply that dansylamide exerts a positive homotropic effect and binding of dansylamide at the allosteric site leads to binding of more dansylamide at the catalytic site. The inhibitor binding to the allosteric site may therefore lead to a either a positive or negative homotropic effect leading to better binding and higher potency or lower binding affinity therefore lower potency at the catalytic site.

Consequently, inhibitors that bind but do not inhibit, such as specs compound 2, might have a negative effect on binding of more inhibitor at the actual catalytic site. Conversely, in inhibitors such as specs compound 10 that may not bind tightly but are potent, there may be a positive homotropic effect and there might be more effective binding at the catalytic site than at the allosteric site.

4.3 Analogs from Dr. James Kiddle

Of the three thioxolone analogs synthesized by Dr.James Kiddle (Figure 8), two of them were shown to be more potent than thioxolone from the results of the esterase assay. Compound 2 was the most potent with an IC_{50} value of 970 nM. The structural modifications of these compounds include addition of an ester at the C6 position of the thioxolone benzene ring. This would make the molecule highly

susceptible to hydrolysis and lead to a hydrolysis product that may also bind to the zinc ion through the oxygen atom.

The Kiddle compounds 2 and 3 are structurally very similar with one difference at the C6 atom where compound 2 forms an ester and compound 3 forms an ether. The difference in CA II inhibition activity shows that inhibitors with an ester group are likely to be more potent that those with an ether group. The lower potency of compound 3 compared to the other two suggests that the carbonyl group on the side chain is important. This carbonyl group may result in a better hydrogen bond donor to effect better binding by increased hydrogen bonding.

4.4 Wright State University Sulfonamides

The sulfonamides from Wright State University resulted in six inhibitors out of the total of nineteen compounds submitted. All the inhibitory sulfonamides had IC_{50} values in the micromolar range and were all within the same order of magnitude. The structures of the inhibitory compounds had two common features that might have contributed to their inhibitory activity. First, they all possessed an ionizable nitrogen atom that was positioned in a very accessible position in an amide group. Secondly, most had an aromatic ring attached to the side chain and this is important in attaching to the highly hydrophobic pocket of the CA II active site.

Most also had halogen atoms attached and this may improve binding to the active site via electrostatic effects. The non-inhibitory compounds lacked the ionizable nitrogen atom and because sulfonamides bind through this atom, they may

be lacking in the anchoring group and may not inhibit CA II. This may have contributed to non-inhibition by compounds 1, 3, 4, 6, 7, 13, 16, 17, 18 and 19. Sulfone groups possess a strong negative charge and possession of two sulfone groups by a compound may not contribute to hydrophobic interactions important at the active site hydrophobic pocket. This may lead to those molecules not being bound and hence non-inhibition by compounds including compounds 1, 3, 4, 6 and 7.

These series of compounds suggested that the amide group contributed favorably in the inhibitor molecules. The carbonyl group next to the ionizable nitrogen could contribute by lowering the pK_a of the amide group allowing the loss of a proton to allow the molecule to bind as an anion. The carbonyl oxygen atom can also participate in hydrogen bonding interactions.

4.5 Enzyme Kinetic Studies

Inhibition studies carried out on thioxolone using Michealis-Menten kinetics revealed a dependence of inhibitor potency on inhibitor concentration. This was evident from the substrate-velocity curves that exhibited a decrease in initial velocity as the inhibitor concentration was increased (Figure 14). A more qualitative assessment was performed using Lineweaver-Burk plots (Figure 15) and the results indicated a decrease in maximal velocity (V_{max}) and increase in concentration of substrate required to achieve half-maximal velocity (K_M) with increase in inhibitor concentration.

The effect of thioxolone on the Michealis-Menten parameters V_{max} and K_M is characteristic of mixed inhibition. Mixed inhibition is a combination of competitive and uncompetitive inhibition and mixed inhibitors bind to the active site. Thioxolone, or its hydrolysis products, therefore functions as a mixed inhibitor, binding to both the enzyme and the enzyme-substrate complex. This could explain the results from the preliminary x-ray crystallography studies that showed the probable existence of more than one thioxolone product binding site at the CA II active site.

4.6 Nuclear Magnetic Resonance and Infrared Spectroscopy

The results from NMR did not seem very conclusive especially in analyzing the hydrolysis product. This could be due to the method of extraction used that led to analysis of only one of the products (polar). The failure to detect the aromatic ring is a consequence of the extraction method and the final product is in methanol which consists of the polar component of the mixture excluding the non-polar benzene ring. However, this can still provide evidence of thioxolone hydrolysis since one potion of the structure, the polar portion, was detected implying a fragmentation of the main structure.

4.7 Liquid Chromatography-Mass Spectroscopy Studies

There is no evidence of thioxolone in the sample suggesting that upon incubation with the enzyme, it undergoes transformations and in its active form is probably a cleavage product. From the behavior of the related compounds, the formation of a dimer from a cleavage product of thioxolone might account for the large *m/z* ratio. Alternatively, this could be a result of the formation of an adduct

between a thioxolone derivative and a component from the solvent or buffer as the initial incubation mixture was in buffer. The buffer contained ions such as sodium sulfate that could be ionized and detected.

4.8 Hydrolysis of Thioxolone

The hydrolysis of thioxolone was found to be accelerated by the presence of CA II (Figure 16). Thioxolone hydrolyses in solution and the extent in the absence of CA II was found to be lower that in the presence of CA II. This is in line with the postulated mechanism that suggests hydrolysis of thioxolone upon binding with CA II. Evidence from the Ellman's reagent test (Figure 13) supported the hypothesis of thioxolone hydrolysis by CA II due to the increase in thiol groups when thioxolone was incubated in the presence of CA II. Based on this, the proposed reaction is thought to proceed as shown in Figure 17 below.

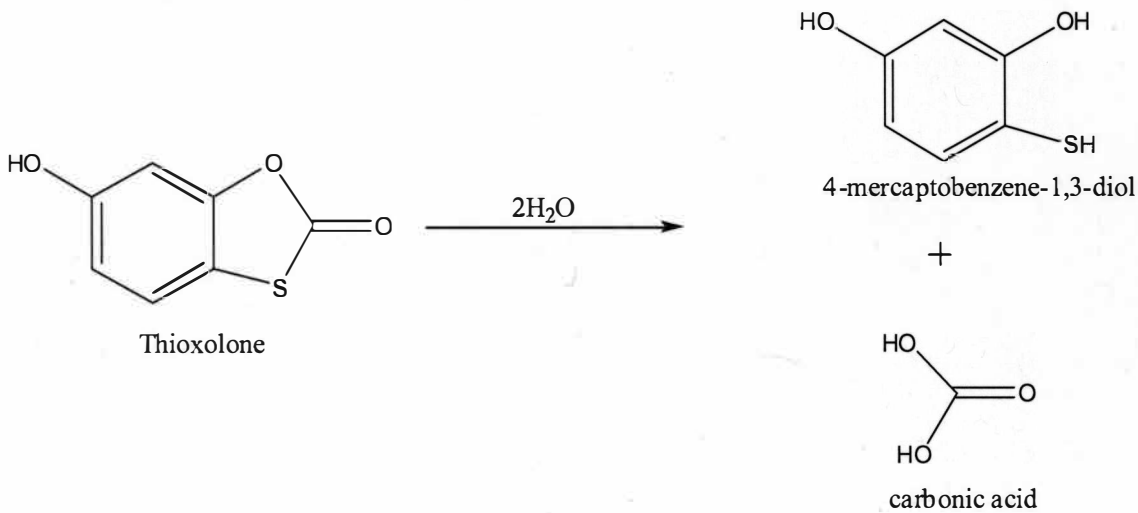

Figure 17. Proposed hydrolysis reaction sequence of thioxolone by CA II

Based on the proposed hydrolysis reaction, the mechanism can be thought to occur as shown in Figure 18 below.

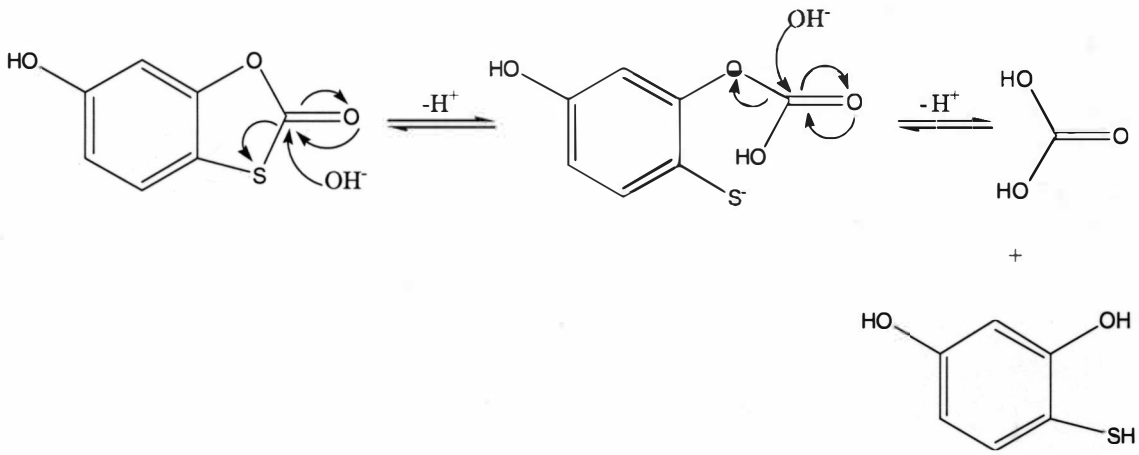

Figure 18. Proposed hydrolysis reaction mechanism of thioxolone by CA II

DTNB can undergo reactions that can result in the formation of the species TNB^{2-} that absorbs strongly at 412 nm and may lead to an overestimation of free thiol formation. These reactions include hydrolysis of the DTNB and nucleophilic attack on DTNB by electrophilic species that may be present in the reaction mixture. Blank measurements of a solution of DTNB and a standard buffer of pH 7.5 containing 50 mM MOPS , 33mM Na_2SO_4 and 33mM EDTA were taken and comparisons were made with the actual reactions mixture. Another blank measurement was made of a solution containing thioxolone, DTNB and the standard MOPS buffer.

This was necessary because thioxolone, being an ester, may undergo hydrolysis in solution and react with DTNB giving rise to the measurable species TNB^{2-} . Comparisons of the blank measurements and the reaction mixture suggested a

hydrolysis of thioxolone by CA II resulting in evolution of the TNB^{2-} species and a free thiol.

4.9 Conclusion

The inhibition of the CA II isozyme has been shown to possess widespread therapeutic potential. For this to be fully utilized, inhibitors need to be developed that can be used under different circumstances. To this end, design of non-sulfonamide CA II inhibitors has not been widely explored. Given the side effects that may be experienced by some segments of the general population, other compounds need to be explored.

In this research, thioxolone, a novel non-sulfonamide molecule with CA II inhibitory potency was investigated together with its analogs using the esterase assay. Its inhibition activity, though weak, could be improved by modifications on the side chains. Inhibitor binding affinity was also investigated using the dansylamide competitive binding assay. Thioxolone's weak binding affinity was found to improve in the analogs upon modification of the side chains with hydrophobic groups and hydrogen-bond acceptors.

Studies attempting to elucidate the mechanism of thioxolone have suggested that it is hydrolyzed and its products may bind to CA II via a thiol linkage. Evidence to support this was exhibited from Ellman's reagent tests and the preliminary x-ray crystallography studies. Results from IR and NMR spectroscopy also suggest hydrolysis of the thioxolone molecule in the presence of CA II. LC-MS studies suggest that thioxolone undergoes structural changes upon binding to CA II and

results in the formation of other molecules distinct from thioxolone. It has been shown that thioxolone is a CA II inhibitor and changes to its structure can be made to greatly improve inhibition activity and binding affinity. Thioxolone hydrolysis products may also have a novel mode of binding CA II via a thiol group.

The molecular details of mechanism and inhibitor binding are important in the process of structure-based drug design. To date, the sulfonamide group accounts for the only functional group incorporated into rationally designed CA II inhibitors for zinc coordination. The exploration of different functional groups capable of binding to the CA II active site may lead to the development of newer and better inhibitors. The discovery of thioxolone and its analogs is a step forward in this direction.

REFERENCES

1. Meldrum, N. & Roughton, F. (1933). Carbonic Anhydrase:Its Preparation and Properties. *Journal of Physiology* **80**, 113-141.
2. Keilin, D. & Mann, T. (1939). Carbonic Anhydrase. *Nature* **144**, 442-443.
3. Khalifah, R. (1971). The Carbon Dioxide Hydration Activity of Carbonic Anhydrase: Stop-Flow Kinetic Studies on the Native Human Isozymes B and C. *Journal of Biological Chemistry* **246**, 2561-2573.
4. Sly, W. & Hu, P. (1995). Human Carbonic Anhydrases and Carbonic Anhydrase Deficiencies. *Annual Review of Biochemistry* **64**, 375-401.
5. Krebs, J., Ippolito, J., Christianson, D. & Fierke, C. (1993). Structural and Functional Importance of a Conserved Hydrogen Bond Network in Human Carbonic Anhydrase II. *Journal of Biological Chemistry* **268**, 27458-27466.
6. Huang, S., Sjoblom, B., Sauer-Eriksson, E. & Jonsson, B. (2002). Organization of an Efficient Carbonic Anhydrase: Implications for the Mechanism Based on Structure-Function Studies of a T199P/C206S Mutant. In *Biochemistry*, Vol. 41, pp. 7628-7635.
7. Christianson, D. & Cox, D. (1999). Catalysis by Metal-Activated Hydroxide in Zinc and Manganese Metalloenzymes. *Annual Review of Biochemistry* **68**, 33-57.
8. Tripp, B., Smith, K. & Ferry, J. (2001). Carbonic Anhydrase:New Insights for an Ancient Enzyme. *Journal of Biological Chemistry* **276**, 48615-48618.
9. Tripp, B., Bell, C., Cruz, F., Krebs, C. & Ferry, J. (2004). A Role for Iron in an Ancient Carbonic Anhydrase. *Journal of Biological Chemistry* **279**, 6683-6687.
10. Chirica, L., Ellenby, B., Jonsson, B. & Lindskog, S. (1997). The complete sequence,expression in *Escherichia coli*,purification and some properties of carbonic anhydrase from *Neisseria Gonorrhoeae*. *European Journal of Biochemistry* **244**, 755-760.
11. Alber, B. & Ferry, J. (1994). A carbonic anhydrase from the archaeon *Methanosarcina thermophila*. *Proceedings of the National Academy of Sciences* **91**, 6909-6913.
12. Pocker, Y. & Stone, J. (1965). The Catalytic versatility of Erythrocyte Carbonic Anhydrase.The Enzyme-Catalyzed Hydrolysis of *p*-Nitrophenyl Acetate. *Journal of the American Chemical Society* **87**, 5497-5498.
13. Pocker, Y. & Sarkanen, S. (1978). Oxonase and Esterase activities of Erythrocyte Carbonic Anhydrase. *Biochemistry* **17**, 1110-1118.
14. Saarnio, J. (2000). Distribution of Carbonic Anhydrase IX,MN/CA IX, in Normal and Neoplastic Gastrointestinal and Hepatobiliary Tissues. Its potential value as a new biomarker and comparison of its expression with that of isozymes I,II,IV, and VI, University of Oulu.

15. Silverman, D. & Lindskog, S. (1988). The Catalytic Mechanism Of Carbonic Anhydrase:Implications of a Rate-Limiting Protolysis of Water. *Accounts of Chemical Research* **21**, 30-36.
16. Supuran, C. T. & Scozzafava, A. (2002). Applications of Carbonic Anhydrase Inhibitors and Activators in Therapy. *Expert Opinion on Therapeutic Patents.* **12**, 217-241.
17. Maren, T. H. (1967). Carbonic Anhydrase:Chemistry,Physiology,and Inhibition. *Physiological Reviews* **47**, 597-765.
18. Scozzafava, A. & Supuran, C. T. (2000). Carbonic Anhydrase Inhibitors and their Therapeutic Potential. *Expert Opinion on Therapeutic Patents.* **10**.
19. Saarnio, J. (2000). Distribution of Carbonic Anhydrase IX,MN/CA IX, in Normal and Neoplastic Gastrointestinal and Hepatobiliary Tissues. Its potential value as a new biomarker and comparison of its expression with that of isozymes I,II,IV, and VI., University of Oulu.
20. Scozzafava, A. & Supuran, C. (2000). Carbonic Anhydrase Inhibitors and their Therapeutic Potential. *Expert Opinion on Therapeutic Patents* **10**.
21. Mann, T. & Keilin, D. (1940). Sulphanilamide as a Specific Inhibitor of Carbonic Anhydrase. *Nature* **146**, 164-165.
22. Epstein, D. & Grant, W. (1977). Carbonic Anhydrase Inhibitor Side Effects.Serum Chemical Analysis. *Archives of Ophthalmology* **95**, 1378-1382.
23. Wallace, T., Fraunfelder, F., Petursson, G. & Epstein, D. (1979). Decreased Libido-A side Effect of Carbonic Anhydrase Inhibitor. *Annals of Ophthalmology* **11**, 1563-1566.
24. Lichter, P. (1981). Reducing Side Effects of Carbonic Anhydrase Inhibitors. *Ophthalmology* **88**, 266-269.
25. Lichter, P., Newman, L., Wheeler, N. & Beall, O. (1978). Patient Tolerance to Carbonic Anhydrase Inhibitors. *American journal of Opthalmology* **85**, 495-502.
26. Saxon, A. & Macy, E. (2004). Cross-reactivity and Sufonamide Antibiotics. *New England Journal of Medicine* **350**, 302-302.
27. Ray, W. (2003). Population-based Studies of Adverse Drug Effects. *New England Journal of Medicine* **349**, 1592-1594.
28. Strom, B., Schinnar, R., Apter, A., Margolis, D., Lautenbach, E., Hennessy, S., Wilker, W. & Pettitt, D. (2003). Absence of Cross-reactivity between Sulfonamide Antibiotics and Sulfonamide Nonantibiotics. *New England Journal of Medicine* **349**, 1628-1635.
29. Davenport, H. (1945). The Inhibition Carbonic Anhydrase by Thiophene-2-Sulfonamide and Sulfanilamide. *Journal of Biological Chemistry* **158**, 567-571.
30. Krebs, H. (1948). Inhibition of carbonic Anhydrase by Sulphonamides. *Biochemical Journal* **43**, 525-528.

31. Miller, W. H., Dessert, A. M. & Roblin, R. O. (1950). Heterocyclic Sulfonamides as carbonic Anhydrase Inhibitors. *Journal of the American Chemical Society* **72**, 4893-4896.
32. Roblin, R. & Clapp, J. (1950). The Preparation of Heterocyclic Sulfonamides. *Journal of the American Chemical Society* **72**, 4890-4892.
33. Maren, T. H. & Conroy, C. W. (1993). A New Class of Carbonic Anhydrase Inhibitor. *Journal of Biological Chemistry* **268**, 26233-26239.
34. Maren, T. (1967). Carbonic Anhydrase:Chemistry,Physiology,and Inhibition. *Physiological Reviews* **47**, 597-765.
35. Maren, T. & Conroy, C. (1993). A New Class of Carbonic Anhydrase Inhibitor. *Journal of Biological Chemistry* **268**, 26233-26239.
36. Supuran, C. & Scozzafava, A. (2002). Applications of Carbonic Anhydrase Inhibitors and Activators in Therapy. *Expert Opinion on Therapeutic Patents* **12**, 217-241.
37. Casini, A., Scozzafava, A., Mincione, F., Menabuoni, L., Ilies, M. & Supuran, C. (2000). Carbonic Anhydrase Inhibitors: Water-Soluble 4-Sulfamoylphenylthioureas as Topical Intraocular Pressure-Lowering Agents with Long-Lasting Effects. *Journal of Medicinal Chemistry* **43**, 4884-4892.
38. Leval, X., Ilies, M., Casini, A., Dogne, J., Scozzafava, A., Masini, E., Mincione, F., Starnotti, M. & Supuran, C. (2004). Carbonic Anhydrase Inhibitors: Synthesis and Topical Intraocular Pressure Lowering Effects of Fluorine-Containing Inhibitors Devoid of Enhanced Reactivity. *journal of Medicinal Chemistry* **47**, 2796-2804.
39. Masereel, B., Rolin, S., Abbate, F., Scozzafava, A. & Supuran, C. T. (2002). Carbonic Anhydrase Inhibitors:Anticonvulsant Sulfonamides Incorporating Valproyl and Other Lipohilic Moeities. *Journal of Medicinal Chemistry* **45**, 312-320.
40. Scozzafava, A., Briganti, F., Ilies, M. & Supuran, C. (2000). Carbonic anhydrase Inhibitors: Synthesis of Membrane-Impermeant Low Molecular weight Sulfonamides Possessing in Vivo Selectivity for the Membrane-Bound versus Cytosolic Isozymes. *Journal of Medicinal Chemistry* **43**, 292-300.
41. Scozzafava, A., Briganti, F., Mincione, G., Menabuoni, L., Mincione, F. & Supuran, C. (1999). Carbonic Anhydrase inhibitors:Synthesis of Water-Soluble, Aminoacyl/Dipeptidyl Sulfonamides Possessing Long-Lasting Intraocular Pressure-Lowering Properties via the Topical Route. *Journal of Medicinal Chemistry* **42**, 3690-3700.
42. Scozzafava, A., Menabuoni, L., Mincione, F., Briganti, F., Mincione, G. & Supuran, C. (1999). Carbonic Anhydrase Inhibitors. Synthesis of Water-Soluble,Topically Effective,Intraocular Pressure-Lowering Aromatic/Heterocyclic Sulfonamides Containing Cationic or Anionic Moeities:Is the Tail More Important than the Ring? *Journal of Medicinal Chemistry* **42**, 2641-2650.

43. Scozzafava, A., Menabuoni, L., Mincione, F., Briganti, F., Mincione, G. & Supuran, C. (2000). Carbonic Anhydrase Inhibitors:Perfluoroalkyl/Aryl-Substituted derivatives of Aromatic/Heterocyclic Sulfonamides as Topical Intraocular Pressure Lowering Agents with Prolonged Duration of Action. *Journal of Medicinal Chemistry* **43**, 4542-4551.

44. Scozzafava, A. & Supuran, C. (2000). Carbonic Anhydrase and Matrix Metalloproteinase Inhibitors: Sulfonylated Amino Acid Hydroxamates with MMP Inhibitory Properties Act as Efficient Inhibitors of CA Isozymes I, II,and IV, and N-Hydroxysulfonamides Inhibit Both These Zinc Enzymes. *Journal of Medicinal Chemistry* **43**, 3677-3687.

45. Lindskog, S. (1997). Structure and Mechanism of Carbonic Anhydrase. *Pharmacology and Therapeutics* **74**, 1-20.

46. Rowlett, R. S., Gargiulo, N. J., Santoli, S. A., Jackson, J. M. & Corbett, A. H. (1991). Activation and Inhibition of Bovine Carbonic anhydrase III by Dianions. *Journal of Biological Chemistry* **266**, 933-941.

47. Pocker, Y. & Stone, J. (1968). The Catalytic Versatility of Erythrocyte Carbonic Anhydrase.VI.Kinetic studies of Noncompetitive Inhibition of *p*-Nitrophenyl Acetate. *Biochemistry* **7**, 2936-2945.

48. Lindskog, S. (1966). Interaction of Cobalt(II)-Carbonic Anhydrase with Anions. *Biochemistry* **5**, 2641-2646.

49. Rowlett, R., Gargiulo, N., Santoli, S., Jackson, J. & Corbett, A. (1991). Activation and Inhibition of Bovine Carbonic anhydrase III by Dianions. *Journal of Biological Chemistry* **266**, 933-941.

50. Simonsson, I., Jonsson, B. & Lindskog, S. (1982). Phenol, A Competitive Inhibitor of CO_2 Hydration Catalyzed by Carbonic Anhydrase. *Biochemical and Biophysical Research Communications* **108**, 1406-1412.

51. Carter, N., Chegwidden, W., Hewett-Emmett, D., Jeffery, S., Shiels, A. & Tashian, R. (1984). Novel Inhibition of Carbonic Anhydrase Isozymes I, II and III by Carbamoyl Phosphate. *FEBS letters* **165**, 197-200.

52. Parr, J. & Khalifah, R. (1992). Inhibition of Carbonic Anhydrases I and II by N-Unsubstituted Carbamate Esters. *Journal of Biological Chemistry* **267**, 25044-25050.

53. Scolnick, L., Clements, M., Liao, J., Crenshaw, L., Hellberg, M., May, J., Dean, T. & Christianson, D. (1997). Novel Binding Mode of Hydroxamate Inhibitors to Human carbonic Anhydrase II. *Journal of the American Chemical Society* **119**, 850-851.

54. Lo, S., Nolan, J., Maren, T., Welstead, W., Gripshover, D. & Shamblee, D. (1992). Synthesis and Physicochemical Properties of Sulfamate Derivatives as topical Antiglaucoma Agents. *Journal of Medicinal Chemistry* **35**, 4790-4794.

55. Maryanoff, B., McComsey, D., Costanzo, M., Hochman, C., Smith-Swintosky, V. & Shank, R. (2005). Comparison of Sulfamate and Sulfamide

Groups for the Inhibition of Carbonic Anhydrase-II by Using Topiramate as a Structural Platform. *Journal of Medicinal Chemistry* **48**, 1941-1947.

56. Recacha, R., Costanzo, M., Maryanoff, B. & Chattopadhyay, D. (2002). Crystal Structure of Human Carbonic Anhydrase II Complexed with an Anti-Convulsant Sugar Sulphamate. *Biochemical Journal* **361**, 437-441.
57. Byres, M. & Cox, P. (2004). The Supramolecular structure of 6-Hydroxy-1,3-benzoxathiol-2-one (Thioxolone). *Acta Crystallographica* **C60**, o395-o396.
58. Lius, V. & Sennerfeldt, P. (1979). Local Treatment of Acne with Tioxolone. *Lakartidningen* **76**, 39-41.
59. Goeth, H. & Wildfeuer, A. (1969). Antibacterial and Cytostatic Properties of 6-Hydroxy-1,3-benzoxathiol-2-one. *Arzneimittelforschung.* **19**, 1298-1304.
60. Wildfeuer, A. (1970). 6-Hydroxy-1,3-benzoxathiol-2-one,An Antipsoriatic with Antibacterial and Antimycotic Properties. *Arzneimittelforschung* **20**, 824-831.
61. Camarasa, J. (1981). Contract Dermatitis toThioxolone. *Contract Dermatitis* **7**, 213-214.
62. Banerjee, A., Swanson, M., Roy, B., Jia, X., Haldar, M., Mallik, S. & Srivastava, D. (2004). Protein Surface-Assisted Enhancement for Recombinant Human Carbonic Anhydrase II. *Journal of the American Chemical Society* **126**, 10875-10883.
63. Chen, R. & Kernohan, J. (1967). Combination of Bovine Carbonic Anhydrase with a Fluorescent Sulfonamide. *Journal of Biological Chemistry* **242**, 5813-5823.
64. Baird, T., Waheed, A., Okuyama, T., Sly, W. & Fierke, C. (1997). Catalysis and Inhibition of Human Carbonic Anhydrase IV. *Biochemistry* **36**, 2669-2678.
65. Ellman, G. (1959). Tissue Sulfhydryl Groups. *Archives of Biochemistry and Biophysics* **82**, 70-77.
66. Riddles, P., Blakeley, R. & Zerner, B. (1983). Reassessment of Ellman's Reagent. *Methods in Enzymology* **91**, 49-60.
67. Grimshaw, C., Whistler, R. & Cleland, W. (1979). Ring Opening and Closing Rates for Thiosugars. *Journal of the American Chemical Society* **101**, 15211532.
68. Voet, D. & Voet, J. (1995). *Biochemistry*. Second edit, Wiley.
69. Wessel, D. & Flugge, U. (1984). A Method for the Quantitative Recovery of Protein in Dilute Solution in the presence of Detergents and Lipids. *Analytical Biochemistry* **138**, 141-143.
70. Cox, D., Hunt, J., Compher, K., Fierke, C. & Christianson, D. (2000). Structural Influence of Hydrophobic Core Residues on Metal Binding and Specificity in Carbonic Anhydrase II. *Biochemistry* **39**, 13687-13694.

71. Yamashita, M., Wesson, L., Eisenman, G. & Eisenberg, D. (1990). Where Metal Ions Bind in Proteins. *Proceedings of the National Academy of Sciences* **87**, 5648-5652.

Appendix A

IC_{50} Curves of Inhibitor Compounds

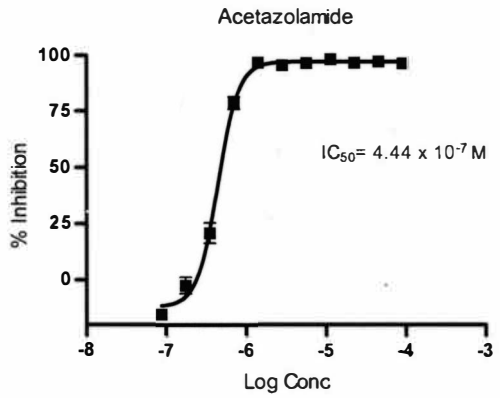

Best-fit values	
BOTTOM	-11.9
TOP	97.24
LOGEC50	-6.352
HILLSLOPE	3.335
IC50	4.44E-07
Std. Error	
BOTTOM	2.032
TOP	0.9206
LOGIC50	0.01309
HILLSLOPE	0.2669
95% Confidence Intervals	
BOTTOM	-16.17 to -7.629
TOP	95.31 to 99.18
LOGIC50	-6.380 to -6.325
HILLSLOPE	2.774 to 3.895
IC50	4.1701e-007 to 4.7330e-007
Goodness of Fit	
Degrees of Freedom	18
R^2	0.9951
Absolute Sum of Squares	197.6
Sy.x	3.313
Data	
Number of X values	11
Number of Y replicates	2
Total number of values	22
Number of missing values	0

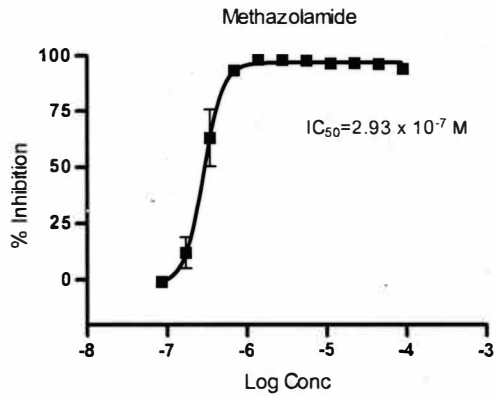

Best-fit values	
BOTTOM	-1.665
TOP	96.59
LOGEC50	-6.534
HILLSLOPE	3.598
IC50	2.93E-07
Std. Error	
BOTTOM	4.254
TOP	1.314
LOGIC50	0.02464
HILLSLOPE	0.6095
95% Confidence Intervals	
BOTTOM	-10.60 to 7.273
TOP	93.83 to 99.35
LOGIC50	-6.585 to -6.482
HILLSLOPE	2.317 to 4.878
IC50	2.5974e-007 to 3.2967e-007
Goodness of Fit	
Degrees of Freedom	18
R^2	0.9833
Absolute Sum of Squares	453.8
Sy.x	5.021
Data	
Number of X values	11
Number of Y replicates	2
Total number of values	22
Number of missing values	0

Thioxolone

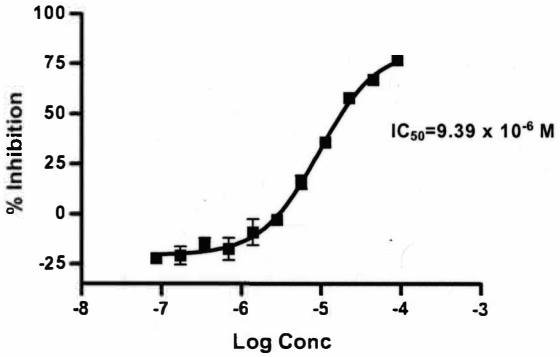

Best-fit values	
BOTTOM	-20.59
TOP	81.86
LOGEC50	-5.027
HILLSLOPE	1.207
EC50	9.39E-06
Std. Error	
BOTTOM	1.883
TOP	4.785
LOGEC50	0.04928
HILLSLOPE	0.1428
95% Confidence Intervals	
BOTTOM	-24.55 to -16.63
TOP	71.81 to 91.92
LOGEC50	-5.131 to -4.924
HILLSLOPE	0.9067 to 1.507
EC50	7.3972e-006 to 1.1916e-005
Goodness of Fit	
Degrees of Freedom	18
R^2	0.9889
Absolute Sum of Squares	316.1
Sy.x	4.19
Data	
Number of X values	11
Number of Y replicates	2
Total number of values	22
Number of missing values	0

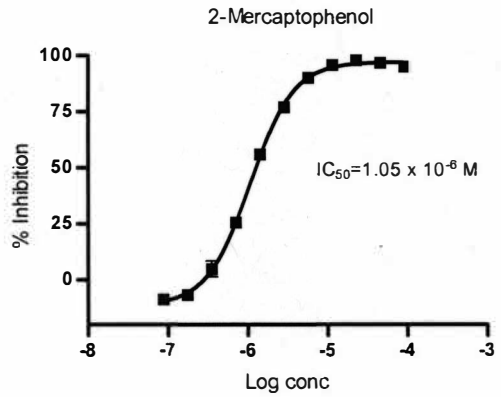

Best-fit values	
BOTTOM	-11.45
TOP	96.96
LOGIC50	-5.977
HILLSLOPE	1.595
IC50	1.05E-06
Std. Error	
BOTTOM	1.426
TOP	0.7734
LOGIC50	0.0141
HILLSLOPE	0.07374
95% Confidence Intervals	
BOTTOM	-14.45 to -8.452
TOP	95.33 to 98.58
LOGIC50	-6.007 to -5.947
HILLSLOPE	1.440 to 1.750
IC50	9.8474e-007 to 1.1287e-006
Goodness of Fit	
Degrees of Freedom	18
R^2	0.9982
Absolute Sum of Squares	72.96
Sy.x	2.013
Data	
Number of X values	11
Number of Y replicates	2
Total number of values	22
Number of missing values	0

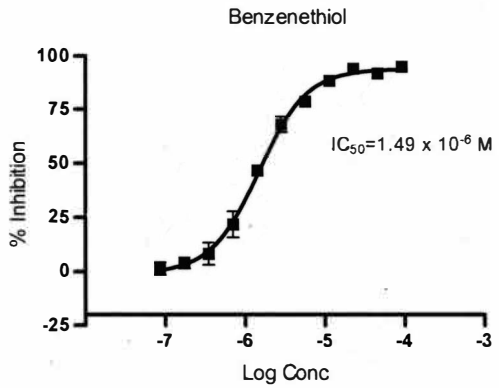

Best-fit values	
BOTTOM	-0.7086
TOP	93.62
LOGEC50	-5.826
HILLSLOPE	1.444
IC50	1.49E-06
Std. Error	
BOTTOM	2.479
TOP	1.641
LOGIC50	0.03162
HILLSLOPE	0.1408
95% Confidence Intervals	
BOTTOM	-5.918 to 4.501
TOP	90.17 to 97.07
LOGIC50	-5.892 to -5.759
HILLSLOPE	1.148 to 1.740
IC50	1.2817e-006 to 1.7405e-006
Goodness of Fit	
Degrees of Freedom	18
R^2	0.9917
Absolute Sum of Squares	250.2
Sy.x	3.729
Data	
Number of X values	11
Number of Y replicates	2
Total number of values	22
Number of missing values	0

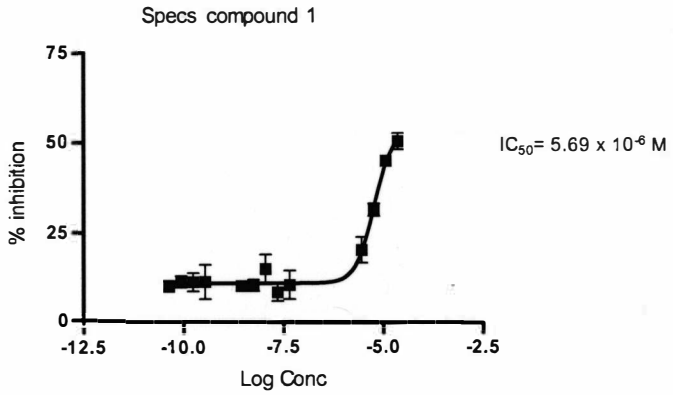

Best-fit values	
BOTTOM	10.79
TOP	53.31
LOGIC50	-5.245
HILLSLOPE	1.899
IC50	5.69E-06
Std. Error	
BOTTOM	0.7852
TOP	4.599
LOGIC50	0.07626
HILLSLOPE	0.5165
95% Confidence Intervals	
BOTTOM	9.163 to 12.42
TOP	43.77 to 62.85
LOGIC50	-5.403 to -5.086
HILLSLOPE	0.8276 to 2.970
IC50	3.9563e-006 to 8.1966e-006
Goodness of Fit	
Degrees of Freedom	22
R^2	0.9513
Absolute Sum of Squares	244.4
Sy.x	3.333
Data	
Number of X values	22
Number of Y replicates	2
Total number of values	26
Number of missing values	18

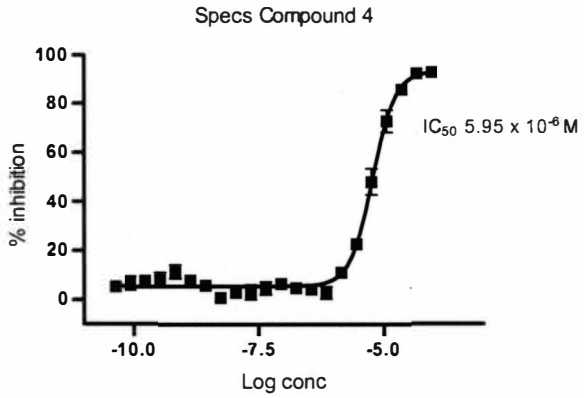

Best-fit values	
BOTTOM	5.546
TOP	93.06
LOGIC50	-5.225
HILLSLOPE	1.899
IC50	5.95E-06
Std. Error	
BOTTOM	0.6435
TOP	1.888
LOGIC50	0.02357
HILLSLOPE	0.1662
95% Confidence Intervals	
BOTTOM	4.264 to 6.828
TOP	89.30 to 96.82
LOGIC50	-5.272 to -5.178
HILLSLOPE	1.568 to 2.230
EC50	5.3407e-006 to 6.6298e-006
Goodness of Fit	
Degrees of Freedom	84
R^2	0.9766
Absolute Sum of Squares	2040
Sy.x	4.928
Data	
Number of X values	22
Number of Y replicates	4
Total number of values	88
Number of missing values	0

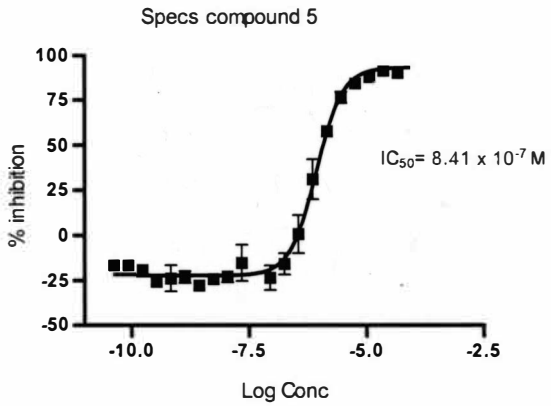

Best-fit values	
BOTTOM	-21.76
TOP	93.38
LOGIC50	-6.075
HILLSLOPE	1.535
IC50	8.41E-07
Std. Error	
BOTTOM	1.477
TOP	2.462
LOGIC50	0.03597
HILLSLOPE	0.169
95% Confidence Intervals	
BOTTOM	-24.75 to -18.77
TOP	88.39 to 98.36
LOGIC50	-6.148 to -6.002
HILLSLOPE	1.193 to 1.878
IC50	7.1115e-007 to 9.9464e-007
Goodness of Fit	
Degrees of Freedom	38
R^2	0.983
Absolute Sum of Squares	1744
Sy.x	6.774
Data	
Number of X values	22
Number of Y replicates	2
Total number of values	42
Number of missing values	2

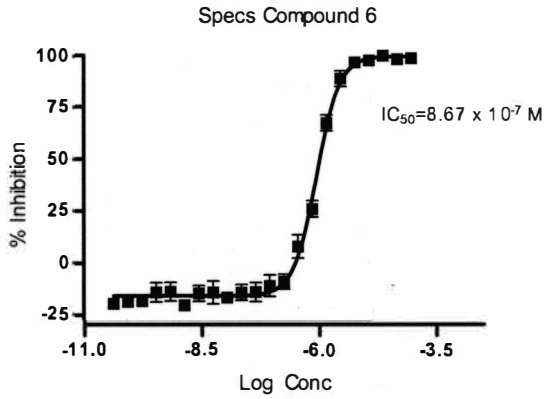

Best-fit values	
BOTTOM	-15.76
TOP	99.55
LOGIC50	-6.062
HILLSLOPE	1.769
IC50	8.67E-07
Std. Error	
BOTTOM	0.9768
TOP	1.635
LOGIC50	0.02263
HILLSLOPE	0.1411
95% Confidence Intervals	
BOTTOM	-17.70 to -13.81
TOP	96.29 to 102.8
LOGIC50	-6.107 to -6.017
HILLSLOPE	1.488 to 2.050
EC50	7.8154e-007 to 9.6184e-007
Goodness of Fit	
Degrees of Freedom	84
R^2	0.9827
Absolute Sum of Squares	3765
Sy.x	6.695
Data	
Number of X values	22
Number of Y replicates	4
Total number of values	88
Number of missing values	0

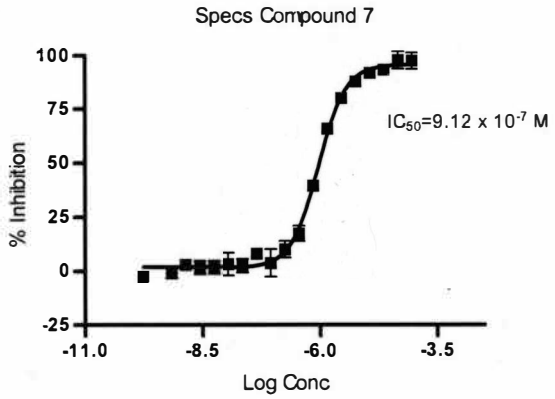

Best-fit values	
BOTTOM	1.919
TOP	95.61
LOGIC50	-6.04
HILLSLOPE	1.477
IC50	9.12E-07
Std. Error	
BOTTOM	1.058
TOP	1.611
LOGIC50	0.02912
HILLSLOPE	0.1274
95% Confidence Intervals	
BOTTOM	-0.1924 to 4.030
TOP	92.39 to 98.82
LOGIC50	-6.098 to -5.982
HILLSLOPE	1.223 to 1.731
IC50	7.9789e-007 to 1.0428e-006
Goodness of Fit	
Degrees of Freedom	72
R^2	0.9789
Absolute Sum of Squares	2636
Sy.x	6.05
Data	
Number of X values	22
Number of Y replicates	4
Total number of values	76
Number of missing values	12

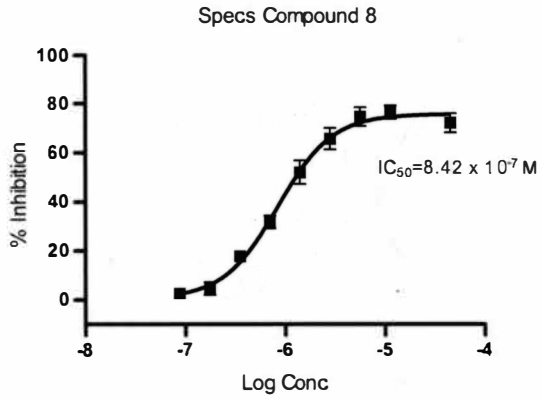

Best-fit values	
BOTTOM	0.9457
TOP	75.81
LOGIC50	-6.075
HILLSLOPE	1.594
IC50	8.42E-07
Std. Error	
BOTTOM	3.722
TOP	2.334
LOGIC50	0.04973
HILLSLOPE	0.2691
95% Confidence Intervals	
BOTTOM	-6.638 to 8.530
TOP	71.05 to 80.56
LOGIC50	-6.176 to -5.973
HILLSLOPE	1.046 to 2.143
EC50	6.6658e-007 to 1.0630e-006
Goodness of Fit	
Degrees of Freedom	32
R^2	0.9566
Absolute Sum of Squares	1327
Sy.x	6.441
Data	
Number of X values	22
Number of Y replicates	4
Total number of values	36
Number of missing values	52

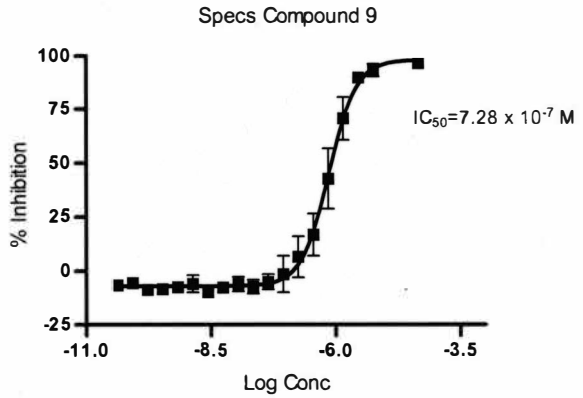

Best-fit values	
BOTTOM	-6.897
TOP	97.56
LOGIC50	-6.138
HILLSLOPE	1.569
IC50	7.28E-07
Std. Error	
BOTTOM	1.557
TOP	4.153
LOGIC50	0.04802
HILLSLOPE	0.2242
95% Confidence Intervals	
BOTTOM	-10.00 to -3.790
TOP	89.27 to 105.9
LOGIC50	-6.233 to -6.042
HILLSLOPE	1.122 to 2.017
IC50	5.8418e-007 to 9.0833e-007
Goodness of Fit	
Degrees of Freedom	72
R^2	0.9345
Absolute Sum of Squares	7698
Sy.x	10.34
Data	
Number of X values	22
Number of Y replicates	4
Total number of values	76
Number of missing values	12

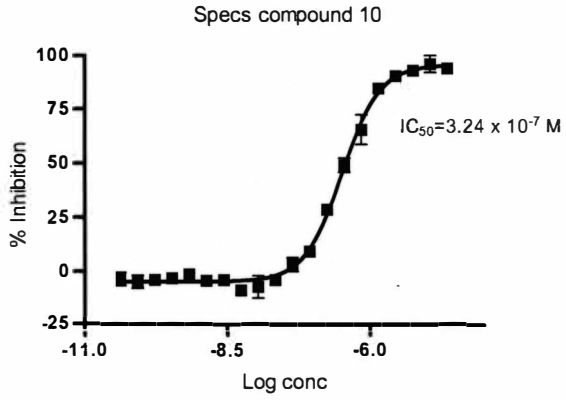

Best-fit values	
BOTTOM	-4.759
TOP	95
LOGIC50	-6.489
HILLSLOPE	1.308
IC50	3.24E-07
Std. Error	
BOTTOM	0.9149
TOP	1.707
LOGIC50	0.02811
HILLSLOPE	0.09631
95% Confidence Intervals	
BOTTOM	-6.584 to -2.935
TOP	91.59 to 98.40
LOGIC50	-6.545 to -6.433
HILLSLOPE	1.116 to 1.500
EC50	2.8490e-007 to 3.6882e-007
Goodness of Fit	
Degrees of Freedom	76
R^2	0.9827
Absolute Sum of Squares	2332
Sy.x	5.539
Data	
Number of X values	22
Number of Y replicates	4
Total number of values	80
Number of missing values	8

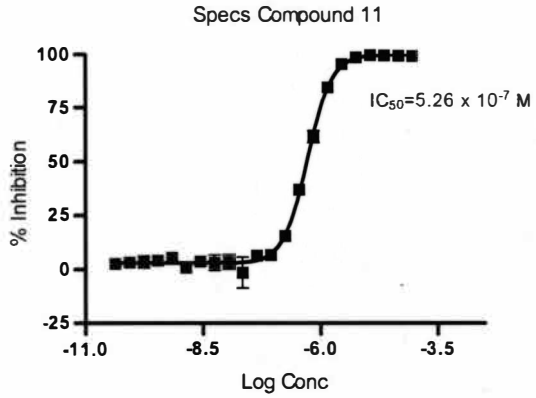

Best-fit values	
BOTTOM	2.952
TOP	99.87
LOGIC50	-6.279
HILLSLOPE	1.684
IC50	5.26E-07
Std. Error	
BOTTOM	0.7123
TOP	1.077
LOGIC50	0.0193
HILLSLOPE	0.1093
95% Confidence Intervals	
BOTTOM	1.533 to 4.371
TOP	97.73 to 102.0
LOGIC50	-6.318 to -6.241
HILLSLOPE	1.466 to 1.901
IC50	4.8124e-007 to 5.7442e-007
Goodness of Fit	
Degrees of Freedom	84
R^2	0.9884
Absolute Sum of Squares	1854
Sy.x	4.698
Data	
Number of X values	22
Number of Y replicates	4
Total number of values	88
Number of missing values	0

Specs Compound 13

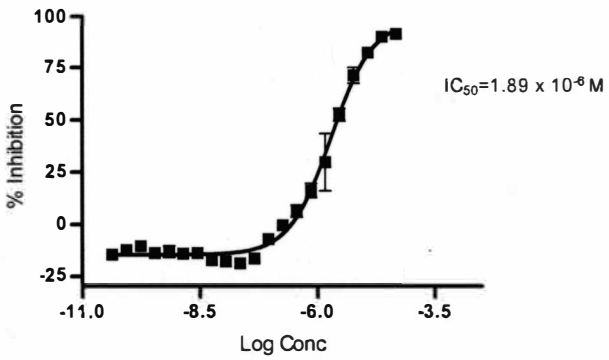

Best-fit values	
BOTTOM	-14.6
TOP	98.25
LOGIC50	-5.723
HILLSLOPE	0.977
IC50	1.89E-06
Std. Error	
BOTTOM	1.119
TOP	4.167
LOGIC50	0.05345
HILLSLOPE	0.09149
95% Confidence Intervals	
BOTTOM	-16.83 to -12.37
TOP	89.95 to 106.6
LOGIC50	-5.829 to -5.616
HILLSLOPE	0.7946 to 1.159
EC50	1.4821e-006 to 2.4209e-006
Goodness of Fit	
Degrees of Freedom	80
R^2	0.969
Absolute Sum of Squares	3979
Sy.x	7.053
Data	
Number of X values	22
Number of Y replicates	4
Total number of values	84
Number of missing values	4

IC_{50} Plots of Analogs from Dr. James Kiddle

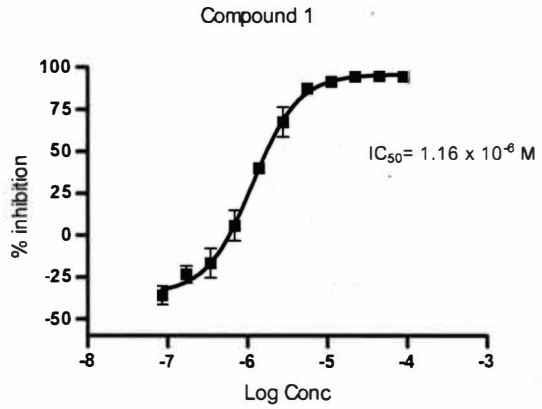

Best-fit values	
BOTTOM	-34.54
TOP	95.43
LOGIC50	-5.935
HILLSLOPE	1.514
IC50	1.16E-06
Std. Error	
BOTTOM	4.895
TOP	2.771
LOGIC50	0.04182
HILLSLOPE	0.1994
95% Confidence Intervals	
BOTTOM	-44.43 to -24.65
TOP	89.83 to 101.0
LOGIC50	-6.020 to -5.851
HILLSLOPE	1.111 to 1.917
IC50	9.5516e-007 to 1.4096e-006
Goodness of Fit	
Degrees of Freedom	40
R^2	0.9675
Absolute Sum of Squares	3770
Sy.x	9.708
Data	
Number of X values	11
Number of Y replicates	4
Total number of values	44
Number of missing values	0

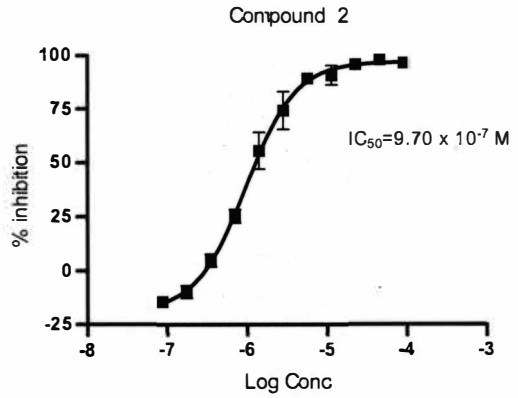

Best-fit values	
BOTTOM	-18.93
TOP	96.79
LOGIC50	-6.013
HILLSLOPE	1.384
IC50	9.70E-07
Std. Error	
BOTTOM	4.894
TOP	2.323
LOGIC50	0.04508
HILLSLOPE	0.1771
95% Confidence Intervals	
BOTTOM	-28.82 to -9.038
TOP	92.10 to 101.5
LOGIC50	-6.105 to -5.922
HILLSLOPE	1.026 to 1.742
IC50	7.8611e-007 to 1.1959e-006
Goodness of Fit	
Degrees of Freedom	40
R^2	0.9699
Absolute Sum of Squares	2525
Sy.x	7.946
Data	
Number of X values	11
Number of Y replicates	4
Total number of values	44
Number of missing values	0

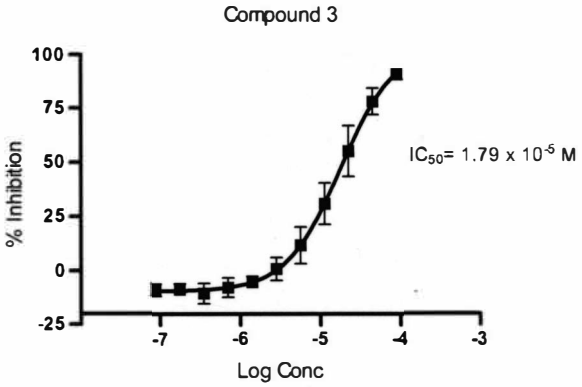

Best-fit values	
BOTTOM	-9.642
TOP	103.8
LOGIC50	-4.747
HILLSLOPE	1.268
IC50	1.79E-05
Std. Error	
BOTTOM	3.104
TOP	14.22
LOGIC50	0.1145
HILLSLOPE	0.2989
95% Confidence Intervals	
BOTTOM	-15.92 to -3.368
TOP	75.06 to 132.6
LOGIC50	-4.978 to -4.515
HILLSLOPE	0.6643 to 1.872
IC50	1.0514e-005 to 3.0522e-005
Goodness of Fit	
Degrees of Freedom	40
R^2	0.9154
Absolute Sum of Squares	5196
Sy.x	11.4
Data	
Number of X values	11
Number of Y replicates	4
Total number of values	44
Number of missing values	0

IC_{50} Plots of Wright State Compounds

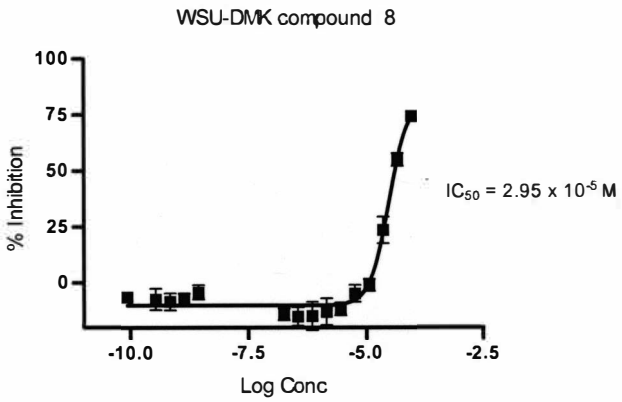

Best-fit values	
BOTTOM	-10.12
TOP	81.9
LOGIC50	-4.53
HILLSLOPE	2.125
IC50	2.95E-05
Std. Error	
BOTTOM	1.23
TOP	8.269
LOGIC50	0.05704
HILLSLOPE	0.4127
95% Confidence Intervals	
BOTTOM	-12.58 to -7.653
TOP	65.33 to 98.48
LOGIC50	-4.644 to -4.415
HILLSLOPE	1.297 to 2.952
IC50	2.2706e-005 to 3.8440e-005
Goodness of Fit	
Degrees of Freedom	56
R^2	0.9213
Absolute Sum of Squares	3415
Sy.x	7.809
Data	
Number of X values	22
Number of Y replicates	4
Total number of values	60
Number of missing values	28

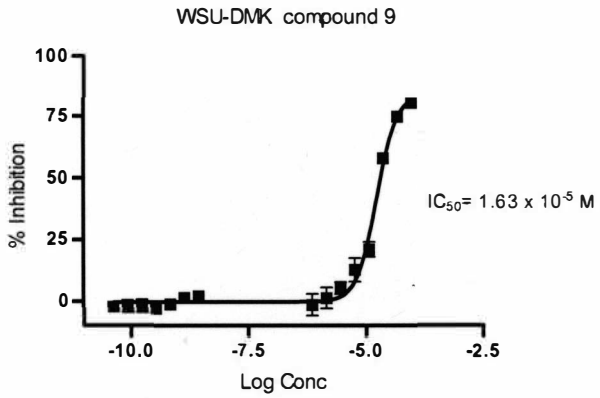

Best-fit values	
BOTTOM	-0.3413
TOP	83.66
LOGIC50	-4.787
HILLSLOPE	2.064
IC50	1.63E-05
Std. Error	
BOTTOM	0.8934
TOP	3.342
LOGIC50	0.03166
HILLSLOPE	0.2484
95% Confidence Intervals	
BOTTOM	-2.132 to 1.449
TOP	76.96 to 90.36
LOGIC50	-4.850 to -4.723
HILLSLOPE	1.566 to 2.561
IC50	1.4123e-005 to 1.8916e-005
Goodness of Fit	
Degrees of Freedom	56
R^2	0.9664
Absolute Sum of Squares	1662
Sy.x	5.448
Data	
Number of X values	22
Number of Y replicates	4
Total number of values	60
Number of missing values	28

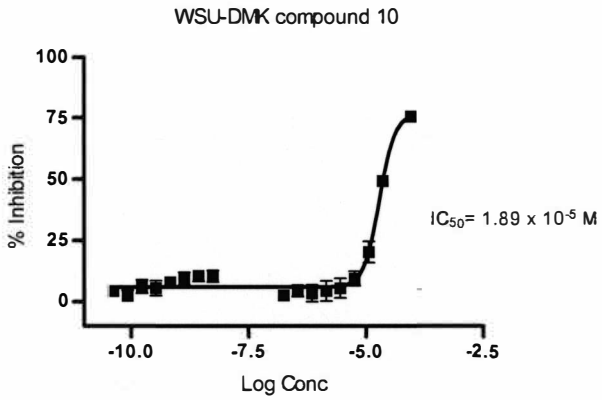

Best-fit values	
BOTTOM	5.988
TOP	76.56
LOGIC50	-4.723
HILLSLOPE	2.613
IC50	1.89E-05
Std. Error	
BOTTOM	0.7715
TOP	3.189
LOGIC50	0.03004
HILLSLOPE	0.4169
95% Confidence Intervals	
BOTTOM	4.446 to 7.530
TOP	70.18 to 82.93
LOGIC50	-4.783 to -4.663
HILLSLOPE	1.780 to 3.446
IC50	1.6467e-005 to 2.1712e-005
Goodness of Fit	
Degrees of Freedom	64
R^2	0.9225
Absolute Sum of Squares	1982
Sy.x	5.564
Data	
Number of X values	22
Number of Y replicates	4
Total number of values	68
Number of missing values	20

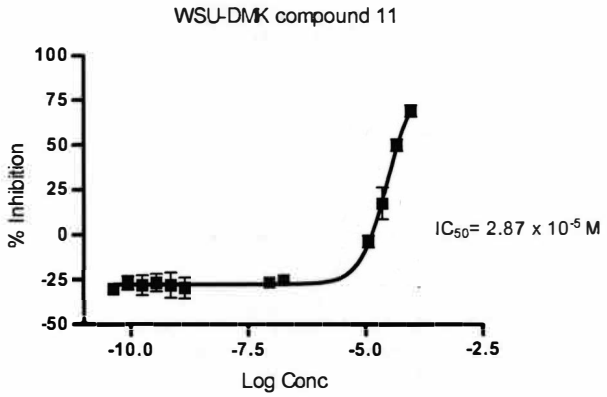

Best-fit values	
BOTTOM	-27.7
TOP	85.89
LOGIC50	-4.542
HILLSLOPE	1.504
IC50	2.87E-05
Std. Error	
BOTTOM	1.494
TOP	15.48
LOGIC50	0.103
HILLSLOPE	0.347
95% Confidence Intervals	
BOTTOM	-30.71 to -24.69
TOP	54.67 to 117.1
LOGIC50	-4.750 to -4.335
HILLSLOPE	0.8044 to 2.204
IC50	1.7782e-005 to 4.6278e-005
Goodness of Fit	
Degrees of Freedom	44
R^2	0.9423
Absolute Sum of Squares	3136
Sy.x	8.442
Data	
Number of X values	22
Number of Y replicates	4
Total number of values	48
Number of missing values	40

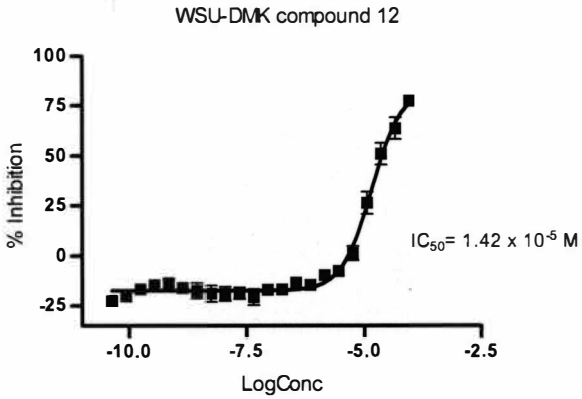

Best-fit values	
BOTTOM	-17.46
TOP	83.63
LOGIC50	-4.847
HILLSLOPE	1.357
IC50	1.42E-05
Std. Error	
BOTTOM	0.8179
TOP	5.516
LOGIC50	0.05318
HILLSLOPE	0.1544
95% Confidence Intervals	
BOTTOM	-19.09 to -15.83
TOP	72.64 to 94.62
LOGIC50	-4.953 to -4.741
HILLSLOPE	1.049 to 1.664
IC50	1.1145e-005 to 1.8153e-005
Goodness of Fit	
Degrees of Freedom	84
R^2	0.9563
Absolute Sum of Squares	3238
Sy.x	6.209
Data	
Number of X values	22
Number of Y replicates	4
Total number of values	88
Number of missing values	0

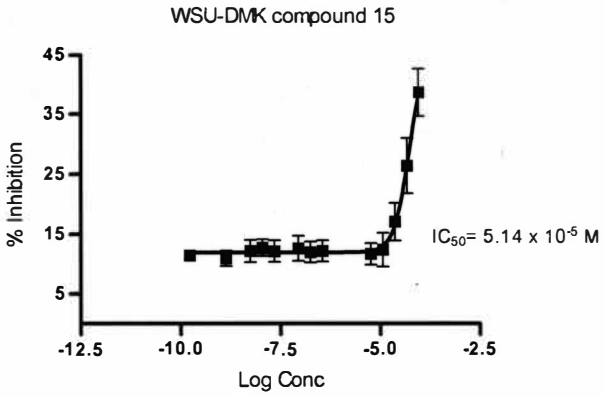

Best-fit values	
BOTTOM	11.94
TOP	46.17
LOGIC50	-4.289
HILLSLOPE	2.25
IC50	5.14E-05
Std. Error	
BOTTOM	0.7544
TOP	12.32
LOGIC50	0.1796
HILLSLOPE	1.068
95% Confidence Intervals	
BOTTOM	10.42 to 13.46
TOP	21.37 to 70.96
LOGIC50	-4.650 to -3.927
HILLSLOPE	0.1003 to 4.399
IC50	2.2370e-005 to 0.0001182
Goodness of Fit	
Degrees of Freedom	48
R^2	0.7622
Absolute Sum of Squares	967.4
Sy.x	4.489
Data	
Number of X values	22
Number of Y replicates	4
Total number of values	52
Number of missing values	36

Appendix B

Dissociation Constant Curves of Specs Compounds

Dissociation Constants

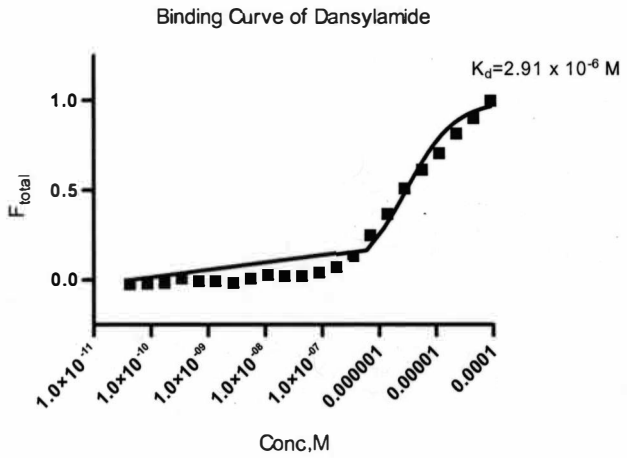

Best-fit values		
Kd	2.91E-06	2.91E-06
Std. Error		
Kd	9.75E-08	9.75E-08
95% Confidence Intervals		
Kd	2.7205e-006 to 3.1029e-006	2.7205e-006 to 3.1029e-006
Goodness of Fit		
Degrees of Freedom		191
R^2	0.9806	0.9806
Absolute Sum of Squares	0.4121	4.12E-01
Sy.x		0.04645
Constraints		
Kd	Kd is shared	
Data		
Number of X values	24	
Number of Y replicates	8	
Total number of values	192	
Number of missing values	0	

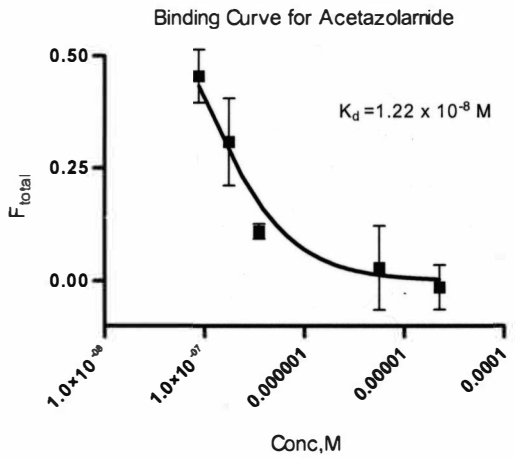

Best-fit values		
Kd	1.22E-08	1.22E-08
Std. Error		
Kd	2.18E-09	2.18E-09
95% Confidence Intervals		
Kd	7.2286e-009 to 1.7094e-008	7.2286e-009 to 1.7094e-008
Goodness of Fit		
Degrees of Freedom		9
R^2	0.836	0.836
Absolute Sum of Squares	0.05929	5.93E-02
Sy.x		0.08117
Constraints		
Kd	Kd is shared	
Data		
Number of X values	11	
Number of Y replicates	2	
Total number of values	10	
Number of missing values	12	

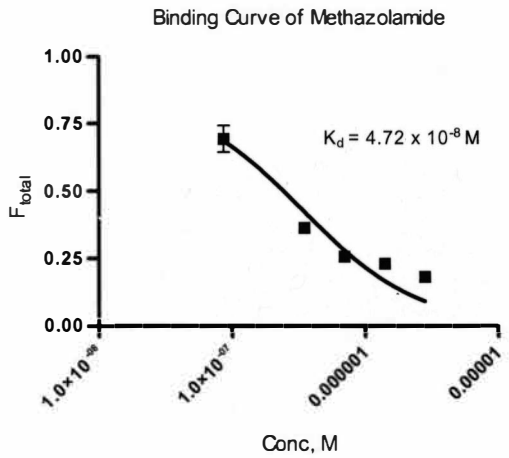

Best-fit values		
Kd	4.72E-08	4.72E-08
Std. Error		
Kd	6.06E-09	6.06E-09
95% Confidence Intervals		
Kd	3.3505e-008 to 6.0901e-008	3.3505e-008 to 6.0901e-008
Goodness of Fit		
Degrees of Freedom		9
R^2	0.8892	0.8892
Absolute Sum of Squares	0.03775	3.78E-02
Sy.x		0.06476
Constraints		
Kd	Kd is shared	
Data		
Number of X values	11	
Number of Y replicates	2	
Total number of values	10	
Number of missing values	12	

Binding Curve for Thioxolone

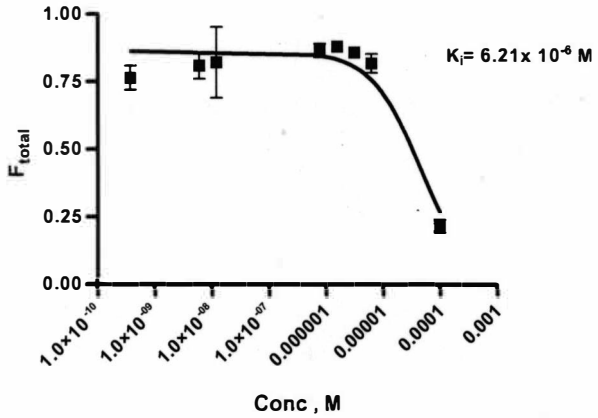

Best-fit values		
Kd	6.21E-06	6.21E-06
Std. Error		
Kd	1.65E-06	1.65E-06
95% Confidence Intervals		
Kd	2.6968e-006 to 9.7328e-006	2.6968e-006 to 9.7328e-006
Goodness of Fit		
Degrees of Freedom		15
R^2	0.8652	0.8652
Absolute Sum of Squares	0.0985	0.0985
Sy.x		0.08103
Constraints		
Kd	KI is shared	
Data		
Number of X values	22	
Number of Y replicates	2	
Total number of values	16	
Number of missing values	28	

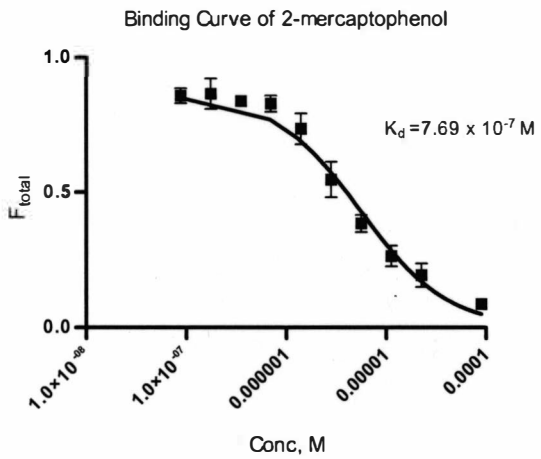

Best-fit values		
Kd	7.69E-07	7.69E-07
Std. Error		
Kd	7.33E-08	7.33E-08
95% Confidence Intervals		
Kd	6.1585e-007 to 9.2267e-007	6.1585e-007 to 9.2267e-007
Goodness of Fit		
Degrees of Freedom		19
R^2	0.9653	0.9653
Absolute Sum of Squares	0.05887	5.89E-02
Sy.x		0.05566
Constraints		
Kd	Kd is shared	
Data		
Number of X values	11	
Number of Y replicates	2	
Total number of values	20	
Number of missing values	2	

Binding Curve of Benzenethiol

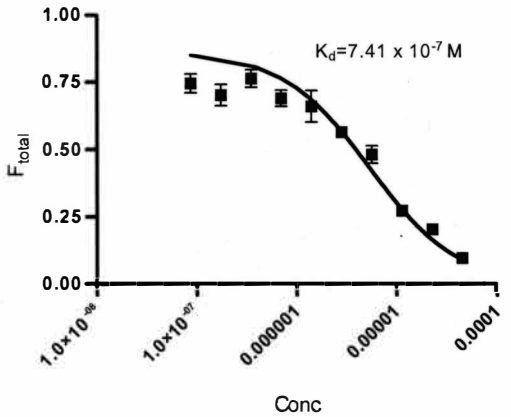

Best-fit values		
Kd	7.41E-07	7.41E-07
Std. Error		
Kd	9.23E-08	9.23E-08
95% Confidence Intervals		
Kd	5.4790e-007 to 9.3410e-007	5.4790e-007 to 9.3410e-007
Goodness of Fit		
Degrees of Freedom		19
R^2	0.9042	0.9042
Absolute Sum of Squares	0.1035	1.04E-01
Sy.x		0.07382
Constraints		
Kd	Kd is shared	
Data		
Number of X values	11	
Number of Y replicates	2	
Total number of values	20	
Number of missing values	2	

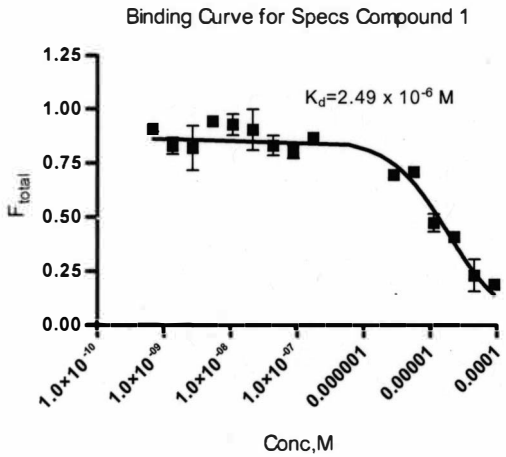

Best-fit values		
Kd	2.49E-06	2.49E-06
Std. Error		
Kd	2.96E-07	2.96E-07
95% Confidence Intervals		
Kd	1.8895e-006 to 3.0993e-006	1.8895e-006 to 3.0993e-006
Goodness of Fit		
Degrees of Freedom		29
R^2	0.9264	0.9264
Absolute Sum of Squares	0.1361	1.36E-01
Sy.x		0.06851
Constraints		
Kd	Kd is shared	
Data		
Number of X values	22	
Number of Y replicates	2	
Total number of values	30	
Number of missing values	14	

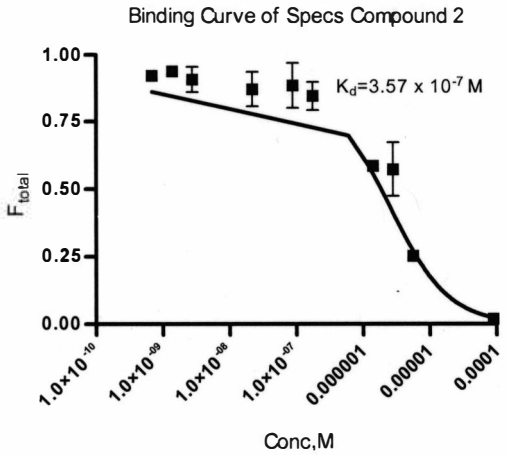

Best-fit values		
Kd	3.57E-07	3.57E-07
Std. Error		
Kd	1.12E-07	1.12E-07
95% Confidence Intervals		
Kd	1.2409e-007 to 5.8934e-007	1.2409e-007 to 5.8934e-007
Goodness of Fit		
Degrees of Freedom		23
R^2	0.8756	0.8756
Absolute Sum of Squares	0.5995	6.00E-01
Sy.x		0.1614
Constraints		
Kd	Kd is shared	
Data		
Number of X values	22	
Number of Y replicates	2	
Total number of values	24	
Number of missing values	20	

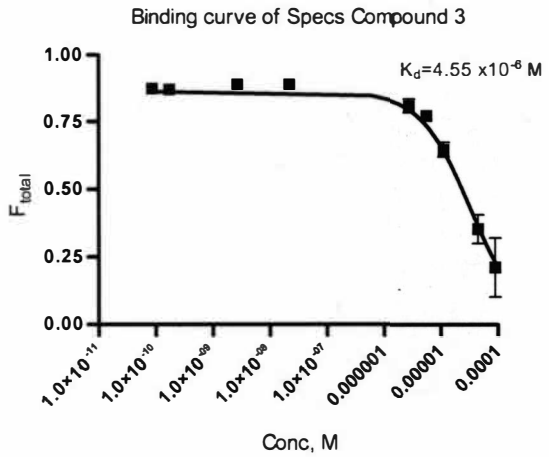

Best-fit values		
Kd	4.55E-06	4.55E-06
Std. Error		
Kd	4.61E-07	4.61E-07
95% Confidence Intervals		
Kd	3.5808e-006 to 5.5252e-006	3.5808e-006 to 5.5252e-006
Goodness of Fit		
Degrees of Freedom		17
R^2	0.962	0.962
Absolute Sum of Squares	0.04006	4.01E-02
Sy.x		0.04854
Constraints		
Kd	Kd is shared	
Data		
Number of X values	22	
Number of Y replicates	2	
Total number of values	18	
Number of missing values	26	

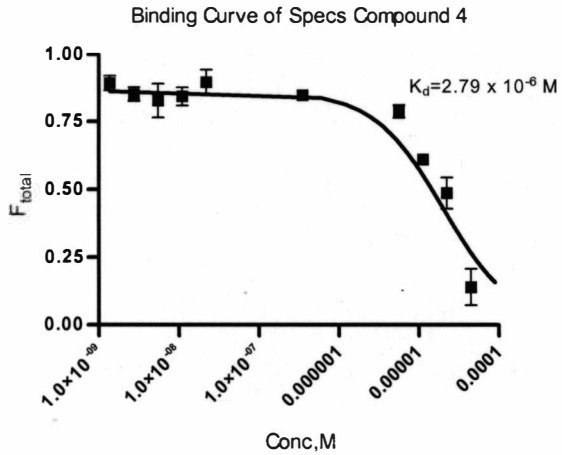

Best-fit values		
Kd	2.79E-06	2.79E-06
Std. Error		
Kd	4.54E-07	4.54E-07
95% Confidence Intervals		
Kd	1.8482e-006 to 3.7348e-006	1.8482e-006 to 3.7348e-006
Goodness of Fit		
Degrees of Freedom		21
R^2	0.915	0.915
Absolute Sum of Squares	0.1746	1.75E-01
Sy.x		0.09119
Constraints		
Kd	Kd is shared	
Data		
Number of X values	22	
Number of Y replicates	2	
Total number of values	22	
Number of missing values	22	

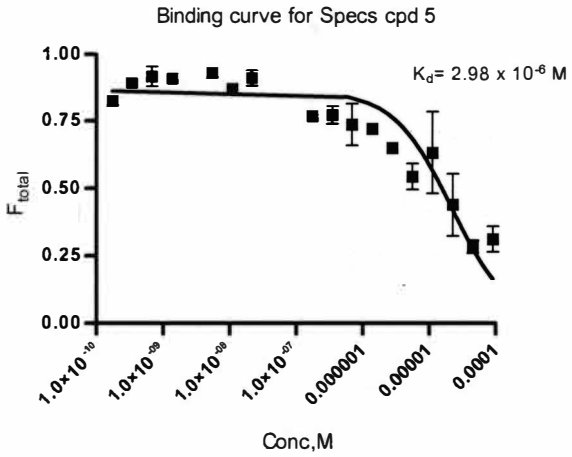

Best-fit values		
Kd	2.98E-06	2.98E-06
Std. Error		
Kd	4.99E-07	4.99E-07
95% Confidence Intervals		
Kd	1.9658e-006 to 3.9959e-006	1.9658e-006 to 3.9959e-006
Goodness of Fit		
Degrees of Freedom		33
R^2	0.7927	0.7927
Absolute Sum of Squares	0.311	3.11E-01
Sy.x		0.09709
Constraints		
Kd	Kd is shared	
Data		
Number of X values	22	
Number of Y replicates	2	
Total number of values	34	
Number of missing values	10	

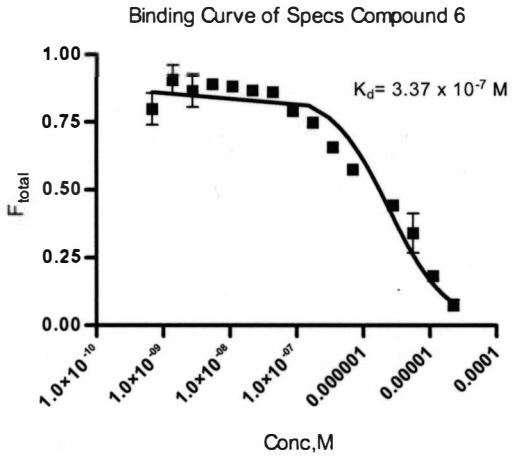

Best-fit values		
Kd	3.37E-07	3.37E-07
Std. Error		
Kd	4.06E-08	4.06E-08
95% Confidence Intervals		
Kd	2.5362e-007 to 4.1962e-007	2.5362e-007 to 4.1962e-007
Goodness of Fit		
Degrees of Freedom		29
R^2	0.9467	0.9467
Absolute Sum of Squares	0.1147	1.15E-01
Sy.x		0.0629
Constraints		
Kd	Kd is shared	
Data		
Number of X values	22	
Number of Y replicates	2	
Total number of values	30	
Number of missing values	14	

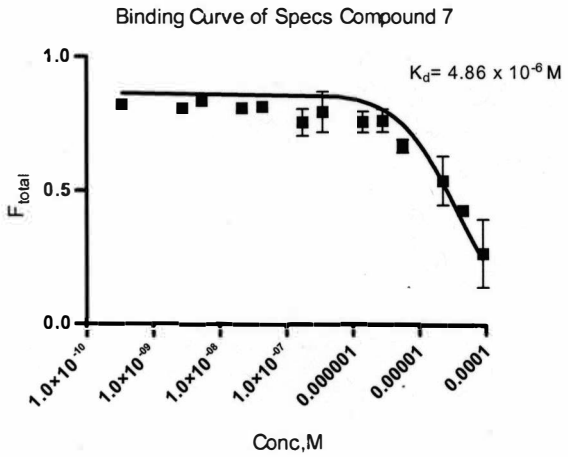

Best-fit values		
Kd	4.86E-06	4.86E-06
Std. Error		
Kd	7.54E-07	7.54E-07
95% Confidence Intervals		
Kd	3.3066e-006 to 6.4131e-006	3.3066e-006 to 6.4131e-006
Goodness of Fit		
Degrees of Freedom		25
R^2	0.8076	0.8076
Absolute Sum of Squares	0.1598	1.60E-01
Sy.x		0.07994
Constraints		
Kd	Kd is shared	
Data		
Number of X values	22	
Number of Y replicates	2	
Total number of values	26	
Number of missing values	18	

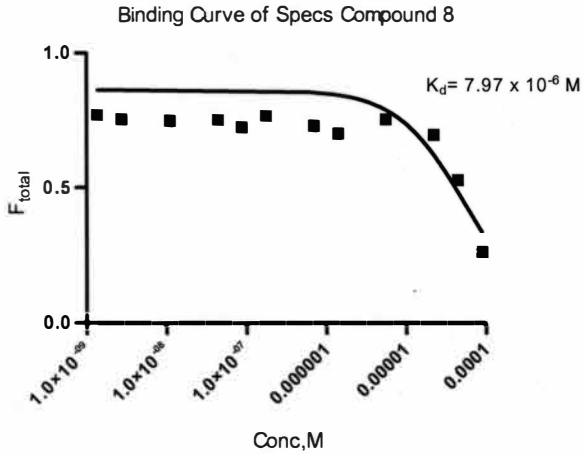

Best-fit values		
Kd	7.97E-06	7.97E-06
Std. Error		
Kd	2.39E-06	2.39E-06
95% Confidence Intervals		
Kd	2.6960e-006 to 1.3237e-005	2.6960e-006 to 1.3237e-005
Goodness of Fit		
Degrees of Freedom		11
R^2	0.4835	0.4835
Absolute Sum of Squares	0.122	1.22E-01
Sy.x		0.1053
Constraints		
Kd	Kd is shared	
Data		
Number of X values	22	
Number of Y replicates	3	
Total number of values	12	
Number of missing values	54	

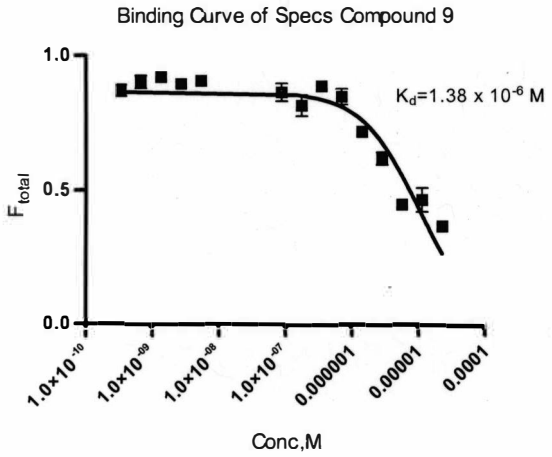

Best-fit values		
Kd	1.38E-06	1.38E-06
Std. Error		
Kd	1.51E-07	1.51E-07
95% Confidence Intervals		
Kd	1.0711e-006 to 1.6916e-006	1.0711e-006 to 1.6916e-006
Goodness of Fit		
Degrees of Freedom		27
R^2	0.9007	0.9007
Absolute Sum of Squares	0.09949	9.95E-02
Sy.x		0.0607
Constraints		
Kd	Kd is shared	
Data		
Number of X values	22	
Number of Y replicates	2	
Total number of values	28	
Number of missing values	16	

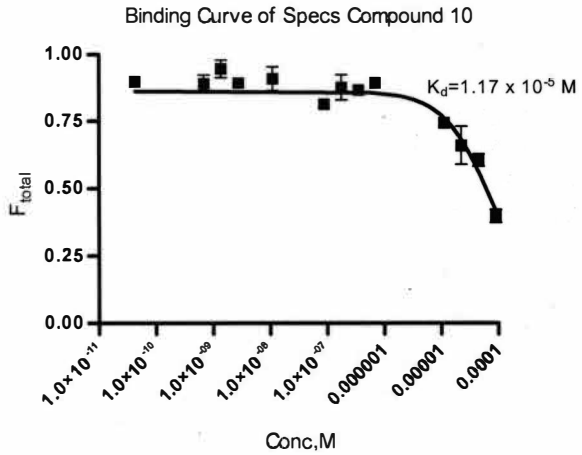

Best-fit values		
Kd	1.17E-05	1.17E-05
Std. Error		
Kd	1.26E-06	1.26E-06
95% Confidence Intervals		
Kd	9.1322e-006 to 1.4322e-005	9.1322e-006 to 1.4322e-005
Goodness of Fit		
Degrees of Freedom		25
R^2	0.8961	0.8961
Absolute Sum of Squares	0.06508	6.51E-02
Sy.x		0.05102
Constraints		
Kd	Kd is shared	
Data		
Number of X values	22	
Number of Y replicates	2	
Total number of values	26	
Number of missing values	18	

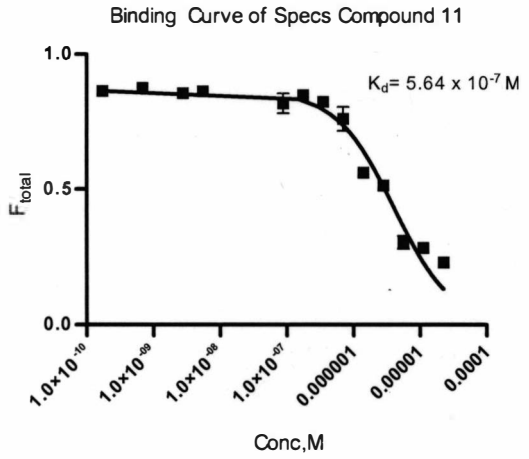

Best-fit values		
Kd	5.64E-07	5.64E-07
Std. Error		
Kd	4.67E-08	4.67E-08
95% Confidence Intervals		
Kd	4.6779e-007 to 6.6031e-007	4.6779e-007 to 6.6031e-007
Goodness of Fit		
Degrees of Freedom		25
R^2	0.9604	0.9604
Absolute Sum of Squares	0.0592	5.92E-02
Sy.x		0.04866
Constraints		
Kd	Kd is shared	
Data		
Number of X values	22	
Number of Y replicates	2	
Total number of values	26	
Number of missing values	18	

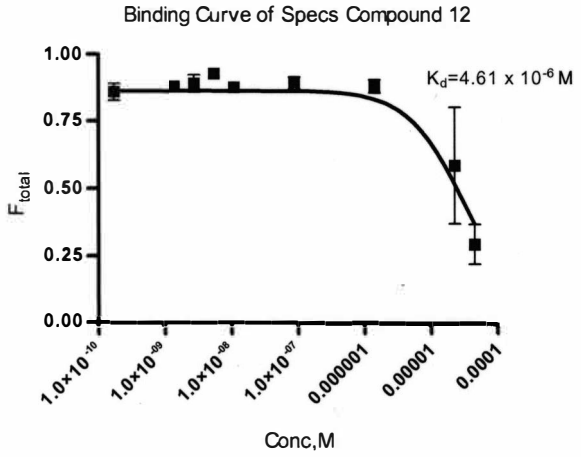

Best-fit values		
Kd	4.61E-06	4.61E-06
Std. Error		
Kd	1.02E-06	1.02E-06
95% Confidence Intervals		
Kd	2.4697e-006 to 6.7533e-006	2.4697e-006 to 6.7533e-006
Goodness of Fit		
Degrees of Freedom		17
R^2	0.8216	0.8216
Absolute Sum of Squares	0.1458	1.46E-01
Sy.x		0.09262
Constraints		
Kd	Kd is shared	
Data		
Number of X values	22	
Number of Y replicates	2	
Total number of values	18	
Number of missing values	26	

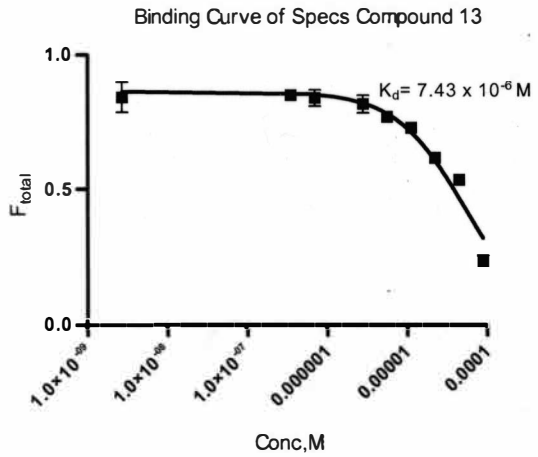

Best-fit values		
Kd	7.43E-06	7.43E-06
Std. Error		
Kd	6.66E-07	6.66E-07
95% Confidence Intervals		
Kd	6.0188e-006 to 8.8314e-006	6.0188e-006 to 8.8314e-006
Goodness of Fit		
Degrees of Freedom		17
R^2	0.942	0.942
Absolute Sum of Squares	0.03865	3.87E-02
Sy.x		0.04768
Constraints		
Kd	Kd is shared	
Data		
Number of X values	22	
Number of Y replicates	2	
Total number of values	18	
Number of missing values	26	

Appendix C

Infrared Spectroscopy Spectra

Infrared Spectroscopy Spectra

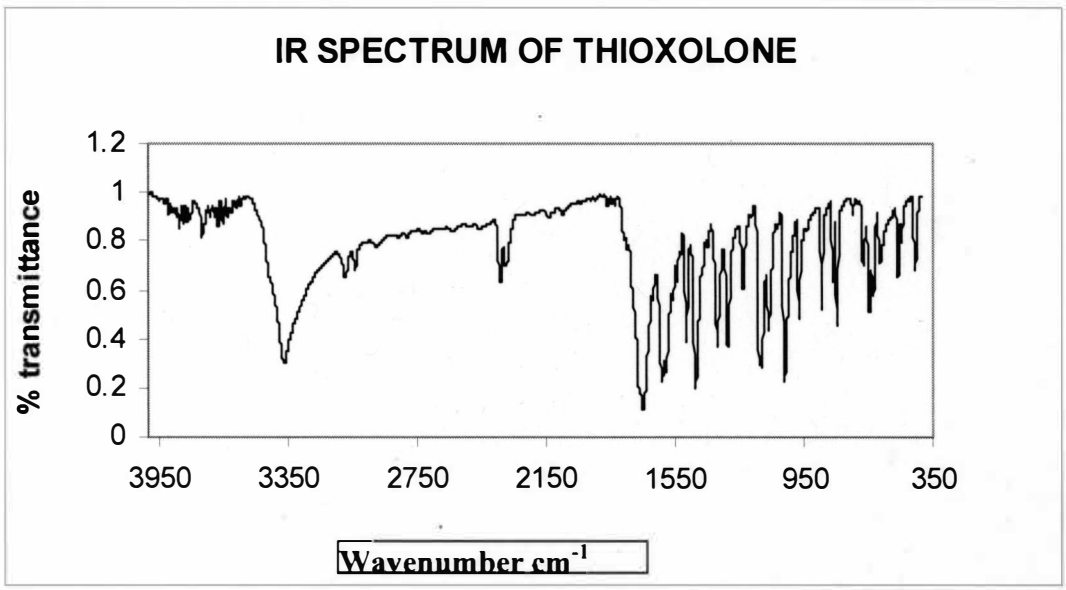

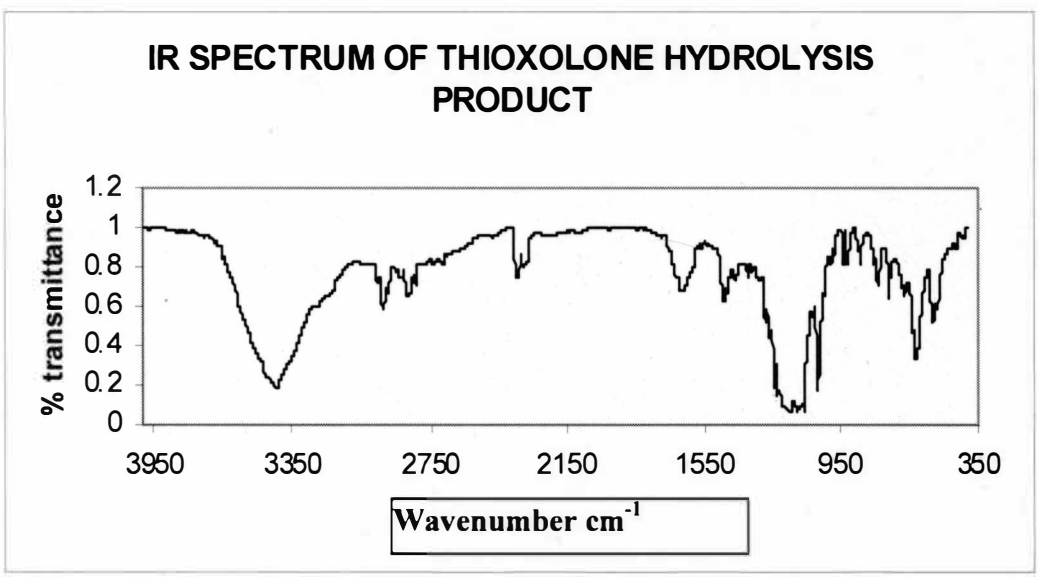

Appendix D

Nuclear Magnetic Resonance Spectroscopy Spectra

Nuclear Magnetic resonance Spectroscopy Spectra

^{1}H NMR OF THIOXOLONE

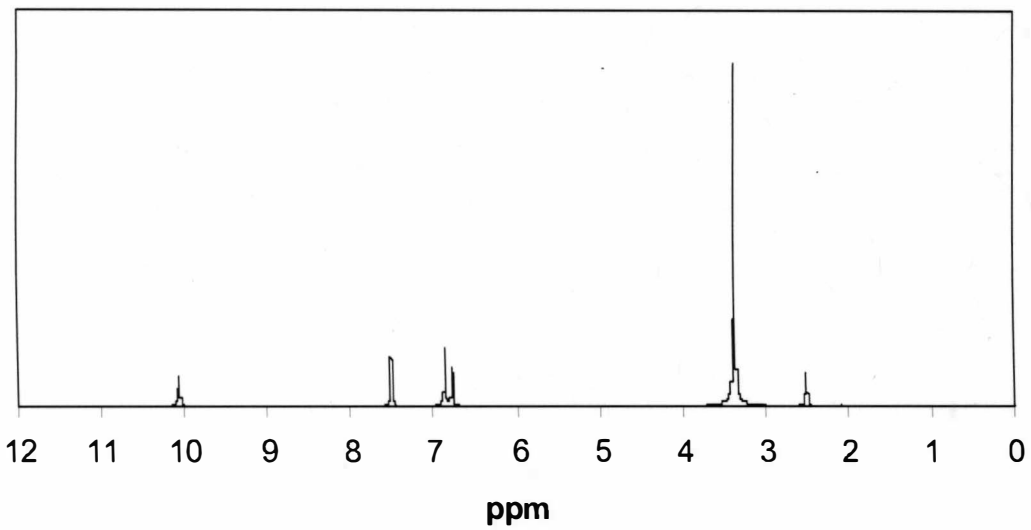

^{1}H NMR SPECTRUM OF THIOXOLONE HYDROLYSIS PRODUCT

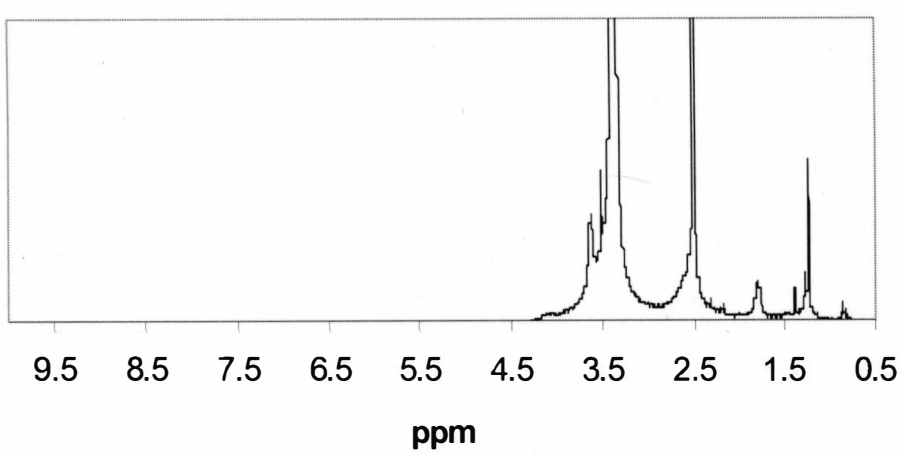

Appendix E

Liquid Chromatography-Mass Spectroscopy Spectra

Thioxolone (negative ionization mode)

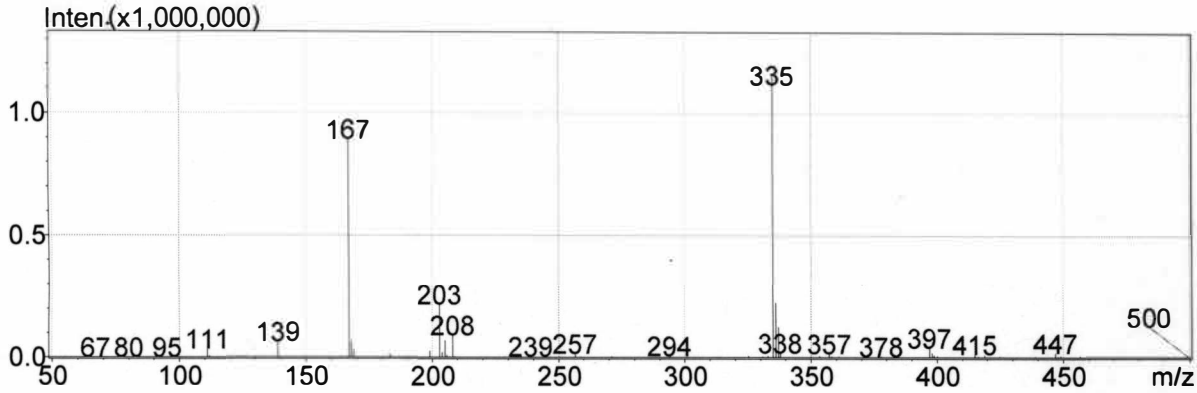

2-Mercaptophenol (negative ionization mode)

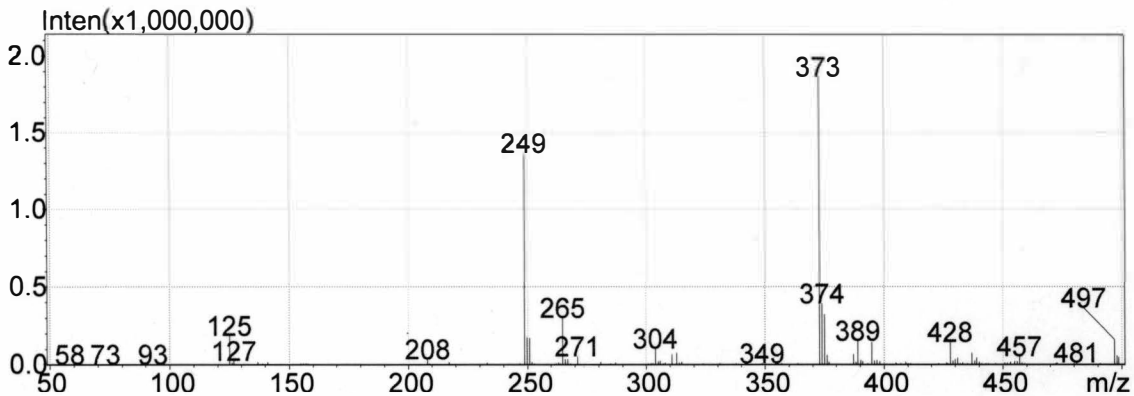

Sample (negative ionization mode)